POLITECNICO DI TORINO
Repository ISTITUZIONALE

Optimal controllability in space of continuum adhesive systems: an a posteriori approach

Original
Optimal controllability in space of continuum adhesive systems: an a posteriori approach / Di Stefano, S., Giammarini, A., Zoppello, M.. - In: ZEITSCHRIFT FUR ANGEWANDTE MATHEMATIK UND PHYSIK. - ISSN 0044-2275. - 77:7(2026), pp. 1-31. [10.1007/s00033-026-02829-2]

Availability:
This version is available at: 11583/3014798 since: 2026-08-24T10:36:56Z

Publisher:
Springer

Published
DOI:10.1007/s00033-026-02829-2

Terms of use:

This article is made available under terms and conditions as specified in the corresponding bibliographic description in the repository

Publisher copyright

(Article begins on next page)

30 October 2026

Z. Angew. Math. Phys. (2026) 77:186
© 2026 The Author(s)
0044-2275/26/070001-31
published online June 17, 2026
https://doi.org/10.1007/s00033-026-02829-2

Zeitschrift für angewandte Mathematik und Physik ZAMP



Optimal controllability in space of continuum adhesive systems: an *a posteriori* approach

Salvatore Di Stefano, Alessandro Giammarini and Marta Zoppello

Abstract. Within the framework of Continuum Mechanics, and building upon Geometric Control Theory, we develop a novel approach to analyze the spatial controllability of deformable media. Here, controllability in space refers to the capability of a continuum body to respond to external stimuli and, in conjunction with internal forces, to modify its shape in order to attain a prescribed target configuration. In detail, we derive the field equations governing the equilibrium of an adhesive system and, following a variational-based procedure, we single out the effects arising from three distinct contributions: (i) internal elastic forces, (ii) internal non-elastic forces, and (iii) external forces. The latter can be treated from two complementary perspectives. One is called *a priori* controllability and relies on the fact that the external force is assigned in advance, by prescribing its functional expression in terms of the system's state and/or to external (mechanical or non-mechanical) factors. On the other hand, we speak of *a posteriori* controllability when the external force is not given at the beginning of the problem but computed in order for the adhesive complex to reach a prescribed deformation. Finally, we demonstrate how fundamental results of Geometric Control Theory can be applied to Continuum Mechanics in a clear and rigorous manner, by interpreting controls as spatial functions that drive a given system adhesive toward configurations characterized by prescribed values of displacement and stress.

Mathematics Subject Classification. 74Cxx, 74Fxx, 34Hxx.

Keywords. Adhesion, Space controllability, *A posteriori* Controllability, Geometric Control Theory, Optimal Control, Theory Shear lag.

1. Introduction

Broadly speaking—and without mention to any specific physical system—the term *adhesion* denotes one of the several mechanisms by which two or more distinct materials are joined and remain connected (see [14,19] and references therein). This concept arises, for example, in the technological context of functional joining, which quotes the process of combining multiple components to design or fabricate structural systems with tailored physical properties and defined performance levels [35]. Similarly, biomechanics reveal how living systems develop adhesive strategies to manage mechanical forces with their surroundings, offering valuable insights for bio-inspired technologies [21,27,30,38].

In this work, we examine adhesion mediated by a glue-like material that binds two deformable media, each possessing its own elastic properties, thereby allowing the transmission of interactions between the two adherents [13]. As a matter of fact, the overall mechanical properties of an adhesive system, as those pertaining to its elastic and structural response, strongly rely upon those of each of its single components and on the way they mutually interact.[1] More specifically, we employ the *shear lag model* [7,13,37], representing one of the most widely used methodologies to study deformable (side-by-side) elements connected by a layer of adherent material. The latter is meant to transfer the loads through shear stresses distributed along the dimension of the bond [7,13,37]. Moreover, if the adherents are relatively rigid, the

[1] Here, the constitutive behavior of the adherends and their mechanical interplay through the adhesive layer.

transfer occurs more uniformly. Conversely, if the adherents are noticeably deformable, significant peaks in their shear stresses will occur at the ends of the joints [7,13,37]. This is evident, for example, in the mechanical response of living cells attached to the extra-cellular matrix (ECM) through focal adhesions (for specific details, both biological and biomechanical, see [3,4]). Furthermore, it has been experimentally proven that the elastic properties of the ECM modulate and regulate the formation, disassemble and stability of focal adhesions themselves [3,4] and these results are reconstructed by mathematical models based on shear lag (see [3,4,26] and references therein). Before going further, we remark that the creation and stabilization of a focal adhesion is a complex phenomenon that depends both on chemical factors (protein complexes, molecular bonding, to name a few) and on mechanical ones (substrate rigidity and the contraction of myosin fibrils [5]). In this regard, a convincing modeling strategy would require at least a chemo-mechanical description, in which both contributions are coupled among themselves, as put forward for example in the works [8,33]. However, in the biological regime in which the adhesion complexes are mature and stable, the mechanical effects are prevalent and their influence is crucial in determining the growth of a focal adhesion and the equilibrium state of the cell [1,32]. Hence, mechanical forces between focal adhesions and the ECM, related to the interactions exchanged by the myosin fibers with the surrounding environment, control the lifetime of focal adhesions themselves. In this sense, the chemical coupling is assumed to be part of such controlling force, that is determined from the outset, instead of being modeled as part of the system.

A similar shear lag approach is also used to mirror the behavior of focal adhesions to grow along a fixed direction (anisotropic growth) and to produce non-elastic forces related to their structural rearrangement [10,26]. On the other hand, adherents of industrial interest, as is the case of double lap joints, is studied in [13,25,31], while we refer to [22,36] for the case of sandwich structures.

1.1. The role of external forces: the *a posteriori* controllability

This work introduces a novel reformulation of a Continuum Mechanics problem—specifically, the one-dimensional deformation of a linear elastic adhesive system—as a spatial control problem. While Control Theory is traditionally applied to dynamical systems governed by a time order parameter, the present study adopts a different perspective by extending its application to deformable mechanical systems, which are instead characterized by space order descriptors. In this framework, whereas time-evolving dynamics aim to steer a system from an initial state to a chosen final one through the control of state variables and velocities, the control of a continuum medium consists in determining how the body deforms from a reference placement to a prescribed target one. Accordingly, the control variables, or control functions, represent generalized forces that drive and accompany the system's deformation. Within this setting, it is not necessary to prescribe the form of such forces a priori, as experimental data or precise constitutive relations between the structural elements of the system may not be readily available. Instead, given a desired final placement, the spatial control framework allows one to infer the distribution of forces responsible for the overall deformation. This approach also represents a clear advancement with respect to [11], where the authors study the controllability of a spatially distributed dynamical system. Although the control problem considered in [11] is nonlinear, it still concerns control in time. In that framework, space does not play the role of an order parameter of the theory, but rather serves as a descriptor of the deformation of a growing body, with time acting as the sole parameter governing the system's dynamics. In contrast, the present work explicitly elects space as the order parameter of the theory. This choice requires the introduction of the notion of space controllability and a corresponding reformulation of standard concepts from Geometric Control Theory within a space-based framework.

More in details, the tools of Geometric Control Theory are applied to describe how the external environment may influence the overall behavior of an adhesive system by exchanging forces, called *external*, with it. Following the line of thought of [11], we delineate two different modeling perspectives along which it is possible to define such external agencies. In particular

1. we speak of *a priori* controllability, when the functional form of the external forces is given in advance. In this sense, they trace experimental evidences or certain phenomenologies, with the modeler having the role of prescribing, at least at minimal level, the interplay between the state variables of the system and the external factors, with the latter being expression of mechanical or non-mechanical processes.
2. we understand the *a posteriori* controllability as the approach for which the shape of the external forces is not given as an input for the description of the system's deformation, but computed by asking the system itself to reach a prescribed target state. Accordingly, the external forces assume the role of control functions that dictate the deformative processes bringing a physical (continuous in our work) system from its reference configuration to a chosen deformed placement.

1.2. Controllability in space

Once the point of view of the *a posteriori* controllability is adopted, we look at the point-wise equilibrium as a problem of Geometric Control Theory. According to the goal of our work, Geometric Control Theory aims at designing control inputs that guide a continuum mechanical system toward a desired (target) state along admissible trajectories, while ensuring robustness to uncertainties, external disturbances, and model inaccuracies [2,6,18,34]. In contrast to the standard time evolution perspective, the present work explores control concepts within the framework of structural systems, rather than dynamical ones. Specifically, we adapt the mathematical tools of Geometric Control Theory to problems governed by equilibrium equations rather than differential equations in time. Our focus is on a structural problem of deformation characterized by a spatial coordinate that serves as the order parameter. The equilibrium equations are a system of ordinary differential equations in space, and the objective is to achieve control in space rather than in time. This means that starting from prescribed boundary conditions, the control inputs are designed so that the system attains a desired configuration. In this setting, admissible solutions correspond to spatial trajectories—curves in the configuration space—that satisfy the controlled equilibrium equations. This spatial notion of controllability thus differs fundamentally from the temporal one: while dynamical control seeks to influence the evolution of a system in time, spatial control aims to shape its configuration in space.

Building on this framework, we extend the analysis to optimal control problems [2,6,18,34] for structural continuum systems. In this context, the aim is twofold. Firstly, to make the system attain a desired configuration starting from a given reference one. Secondly, to also do so optimally, according to a prescribed performance criterion. This criterion is expressed through a cost functional that typically measures, for example, the energy of the system or the deviation of the state from a target configuration and the effort required by the control inputs. The control problem is then formulated as the minimization of this cost functional, subject to the equilibrium constraints of the structural system [2,6,18,34]. To derive necessary conditions for optimality, we make use of the Pontryagin Maximum Principle (PMP), which provides a set of boundary value problems coupling the state and co-state variables through a Hamiltonian system. This principle, originally developed for dynamical systems evolving in time, and successfully used in several applications [23,24], is here reformulated in a spatial setting, offering a powerful theoretical framework to characterize optimal configurations along the spatial domain. Since the structural system under consideration is linear, the analysis naturally specializes to the case of Linear-Quadratic (LQ) optimal control problems, in which the cost functional is quadratic and the governing equations are linear. This class of problems is particularly appealing because it allows for explicit analytical treatment and provides deep insights into the geometric structure of optimal spatial control laws.

1.3. Manuscript organization

The manuscript is organized as follows. In Sect. 2 we derive the balance equations governing the pointwise equilibrium of an adhesive system, by making explicit its constitutive behavior and the expression of both elastic and non-elastic internal contributions (see Sect. 2.2). Moreover, we discuss the way in which such equilibrium equations can be put in the form of a space-independent linear system (we refer again to Sect. 2.2) and in Sect. 2.3 discuss how the non-elastic forces determine a symmetry breaking in space, by adopting a fully variational setting. Section 3 is devoted to the novel formulation of the adhesion problem within the control theory framework, with the introduction of the external forces and, by adopting the *a posteriori* controllability, we formulate the deformation of the adhesive system as a control problem (see Sect. 3.1). In Sect. 4, we recall the main tools of Geometric Control Theory and reframe them in terms of space, by introducing the notion of space controllability and space optimality. In Sect. 5, we apply controllability and optimal control in space to a shear lag problem of adhesion, by also proposing dedicated numerical simulation. Conclusions and future perspectives are collected in Sect. 6, while Appendix A studies the spectral and geometric properties of the matrix representing the obtained linear system.

2. Modeling equations

We present a concise, yet comprehensive overview of the main structural and modeling features governing load transfer mechanisms in adhesive systems. Within a purely mechanical framework, we analyze the internal elastic and non-elastic forces exchanged between two linear elastic adherends, idealized as intrinsically one-dimensional and bonded through an adhesive layer. Finally, we formulate the boundary value problem (BVP) describing the mechanical equilibrium of the entire adhesive assembly and recast it as a system of first-order, linear ordinary differential equations (ODEs). As reported in Sect. 1, we adopt the shear lag model [7,13,37].

2.1. Kinematics of the adhesive system and balance equations

The adhesive system investigated in our work is built by joining two different fiber-like components, or adherends, through a layer of adhesive material, or adhesive core. The two fibers are supposed to be thin and have negligible flexural properties, capable of transmitting high tensile forces while offering little resistance to transverse loads. Moreover, they experience only axial deformation (hence, shear deformation and bending are neglected), so that starting from a straight reference placement, they do remain straight under body and boundary loads, both in displacement or force control. Looking at the adhesive layer, it does not carry any significant axial force and, in our approach, we represent it as a bed of springs contributing with elastic and non-elastic forces. The Reader is referred to a schematic of the considered adhesive system as reported in Fig. 1.

The two straight fibers, the upper and the bottom one, are assumed to be parallel and perfectly bonded over their entire reference length L, which is the same for both. Accordingly, we idealize the system as one-dimensional and model it by a line segment, representing the common axis along which the two fibers are joint. Hence, without loss of generality, we take the open and bounded interval $\mathcal{B} =]0, L[\subset \mathbb{R}$ as the reference placement of the adhesive system as a whole and, hereafter, we use the subscripts "a" and "m" for highlighting that a physical quantity of interest is associated with the upper or the bottom fiber, respectively. Moreover, we say that $\bar{\mathcal{B}} = [0, L]$ is the topological closure of $\mathcal{B}$ (indicated by a superimposed bar).

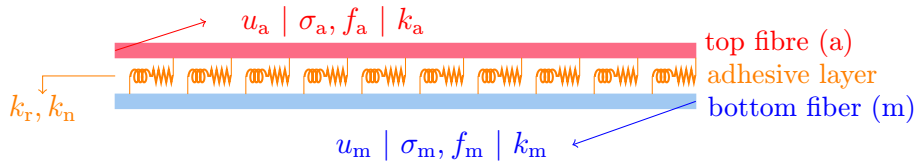


FIG. 1. Schematic of the considered adhesive system, in which we identify the top fiber, the adhesive layer and the bottom fiber. The two types of springs are representative of the elastic (coil spring) and non-elastic (zigzag spring) forces exchanged by the two fibers through the adhesive layer

We denote by $u_a : \bar{\mathcal{B}} \to \mathbb{R}$ and $u_m : \bar{\mathcal{B}} \to \mathbb{R}$ the fibers' displacement fields and introduce the axial deformation fields

$$\varepsilon_a := \frac{du_a}{dx}, \quad \varepsilon_m := \frac{du_m}{dx}, \tag{1}$$

where $x \in \bar{\mathcal{B}}$ is the spatial variable spanning $\bar{\mathcal{B}}$. Finally, if we introduce the fiber's traction fields σ_a and σ_m, as well as the total adhesive forces f_a and f_m (elastic plus non-elastic) exchanged through the adhesive layer, the point-wise equilibrium equations read

$$\frac{d\sigma_a}{dx} + f_a = 0, \qquad \text{in } \mathcal{B}, \tag{2a}$$

$$\frac{d\sigma_m}{dx} + f_m = 0, \qquad \text{in } \mathcal{B}. \tag{2b}$$

In particular, Eqs. (2a) and (2b) are the local forms of the balance of linear momentum for the upper and bottom fibers, respectively.[2]

2.2. Tractions, adhesive forces and final form of the BVP

We complete our modeling framework by assigning constitutively the tractions σ_a and σ_m, i.e., describing the mechanical response of the two fibers through constitutive relations relating σ_a and σ_m to ε_a and ε_m, respectively, declaring the form of the adhesive forces f_a and f_m and setting suitable boundary conditions.

Tractions. We take both the fibers to be linear elastic and, thus, equip the adhesive system with a strain energy density ψ, defined per unit of length, as

$$\psi = \frac{1}{2} k_a \varepsilon_a^2 + \frac{1}{2} k_m \varepsilon_m^2, \tag{3}$$

with k_a and k_m being extensional stiffnesses (physical units of a force). Hence, the constitutive expressions of σ_a and σ_m are obtained by deriving the energy ψ in Eq. (3) with respect to ε_a and ε_m, so that

$$\sigma_a = k_a \varepsilon_a, \quad \sigma_m = k_m \varepsilon_m. \tag{4}$$

We note that since only uniaxial deformation is studied, Eq. (4) represents (the simplest version of) Hook's law for linear elastic materials.

[2] We remark that within the mechanical framework adopted in our work, we do consider only rate independent phenomena, so that Eqs. (2a) and (2b) do not contain any inertial terms.

Elastic and non-elastic forces. We additively split the adhesive forces f_{a} and f_{m} into two terms, i.e.,

$$f_{\mathrm{a}} = f_{\mathrm{a}}^{(\mathrm{el})} + f_{\mathrm{a}}^{(\mathrm{an})}, \qquad f_{\mathrm{m}} = f_{\mathrm{m}}^{(\mathrm{el})} + f_{\mathrm{m}}^{(\mathrm{an})}. \tag{5}$$

In Eq. (5), $f_{\mathrm{a}}^{(\mathrm{el})}$ and $f_{\mathrm{m}}^{(\mathrm{el})}$ account for the elastic forces exchanged by the two fibers through the adhesive layer, here taken proportional to their relative displacement, i.e.,

$$f_{\mathrm{a}}^{(\mathrm{el})} = -\frac{k_{\mathrm{r}}}{d_{\mathrm{r}}}(u_{\mathrm{a}} - u_{\mathrm{m}}), \qquad f_{\mathrm{m}}^{(\mathrm{el})} = \frac{k_{\mathrm{r}}}{d_{\mathrm{r}}}(u_{\mathrm{a}} - u_{\mathrm{m}}), \tag{6}$$

where k_{r} is the elastic rigidity of the adhesive layer (physical units of a force over length) and d_{r} is a characteristic length measuring its thickness (see [4,9,10] for the use of such model to study the elasticity of focal adhesions). We remark that the elastic contributions $f_{\mathrm{a}}^{(\mathrm{el})}$ and $f_{\mathrm{m}}^{(\mathrm{el})}$ are integrable forces, in the sense that they can be obtained from the (quadratic) potential

$$U(u_{\mathrm{a}}, u_{\mathrm{m}}) = -\frac{k_{\mathrm{r}}}{2d_{\mathrm{r}}}(u_{\mathrm{a}} - u_m)^2, \tag{7}$$

by deriving U itself with respect to u_{a} and u_{m}, i.e.,

$$f_{\mathrm{a}}^{(\mathrm{el})} = \frac{\partial U}{\partial u_{\mathrm{a}}}, \quad f_{\mathrm{m}}^{(\mathrm{el})} = \frac{\partial U}{\partial u_{\mathrm{m}}}. \tag{8}$$

On the other hand, the two terms $f_{\mathrm{a}}^{(\mathrm{an})}$ and $f_{\mathrm{m}}^{(\mathrm{an})}$ in Eq. (5) deliver non-elastic contributions and are given as proportional to the relative fibers' deformation, so that

$$f_{\mathrm{a}}^{(\mathrm{an})} = \frac{k_{\mathrm{n}}}{d_{\mathrm{r}}}(\varepsilon_{\mathrm{a}} - \varepsilon_{\mathrm{m}}), \quad f_{\mathrm{m}}^{(\mathrm{an})} = -\frac{k_{\mathrm{n}}}{d_{\mathrm{r}}}(\varepsilon_{\mathrm{a}} - \varepsilon_{\mathrm{m}}), \tag{9}$$

where k_{n} (physical units of a force) is a positive material parameter (see [9,26,29] for this kind of forces introduced in the biomechanical field of cell–matrix interactions). In this case, we look at the Rayleigh-type (quadratic) function [13,20]

$$R(\varepsilon_{\mathrm{a}}, \varepsilon_{\mathrm{m}}) = -\frac{k_{\mathrm{n}}}{2d_{\mathrm{r}}}(\varepsilon_{\mathrm{a}} - \varepsilon_m)^2, \tag{10}$$

and obtain $f_{\mathrm{a}}^{(\mathrm{an})}$ and $f_{\mathrm{m}}^{(\mathrm{an})}$ as derivatives of R with respect to ε_{a} and ε_{m}, respectively, i.e.,

$$f_{\mathrm{a}}^{(\mathrm{an})} = -\frac{\partial R}{\partial \varepsilon_{\mathrm{a}}}, \quad f_{\mathrm{m}}^{(\mathrm{an})} = -\frac{\partial R}{\partial \varepsilon_{\mathrm{m}}}. \tag{11}$$

Final form of the equilibrium equations. By substituting the constitutive relations of Eq. (4), the expressions of $f_{\mathrm{a}}^{(\mathrm{el})}$ and $f_{\mathrm{m}}^{(\mathrm{el})}$ of Eq. (6) and the shape of $f_{\mathrm{a}}^{(\mathrm{an})}$ and $f_{\mathrm{m}}^{(\mathrm{an})}$ of Eq. (9) in Eqs. (2a) and (2b), we obtain the explicit form of the field equations governing the equilibrium of the considered adhesive system as

$$\begin{cases} (k_{\mathrm{a}} u_{\mathrm{a}}')' + \dfrac{k_{\mathrm{n}}}{d_{\mathrm{r}}}(u_{\mathrm{a}}' - u_{\mathrm{m}}') - \dfrac{k_{\mathrm{r}}}{d_{\mathrm{r}}}(u_{\mathrm{a}} - u_{\mathrm{m}}) = 0, & \text{in } \mathcal{B}, \\ (k_{\mathrm{m}} u_{\mathrm{m}}')' - \dfrac{k_{\mathrm{n}}}{d_{\mathrm{r}}}(u_{\mathrm{a}}' - u_{\mathrm{m}}') + \dfrac{k_{\mathrm{r}}}{d_{\mathrm{r}}}(u_{\mathrm{a}} - u_{\mathrm{m}}) = 0, & \text{in } \mathcal{B}, \end{cases} \tag{12}$$

where the apex "′" denotes the derivative with respect to the spatial variable $x \in \bar{\mathcal{B}}$. Assuming all the material parameters appearing in Eq. (12) to be constant (the components of the adhesive system are homogeneous in space) and introduced the notation

$$h = \frac{k_{\mathrm{m}}}{k_{\mathrm{a}}}, \quad h_{\mathrm{n}} = \frac{k_{\mathrm{n}}}{d_{\mathrm{r}} k_{\mathrm{a}}}, \quad h_{\mathrm{r}} = \frac{k_{\mathrm{r}}}{d_{\mathrm{r}} k_{\mathrm{a}}}, \tag{13}$$

where h is non-dimensional, h_{n} has the physical units of the inverse of a length and h_{r} has the dimension of the inverse of an area, we recast Eq. (12) as

$$\begin{cases} u_{\mathrm{a}}'' + h_{\mathrm{n}}(u_{\mathrm{a}}' - u_{\mathrm{m}}') - h_{\mathrm{r}}(u_{\mathrm{a}} - u_{\mathrm{m}}) = 0, & \text{in } \mathcal{B}, \\ u_{\mathrm{m}}'' - \dfrac{h_{\mathrm{n}}}{h}(u_{\mathrm{a}}' - u_{\mathrm{m}}') + \dfrac{h_{\mathrm{r}}}{h}(u_{\mathrm{a}} - u_{\mathrm{m}}) = 0, & \text{in } \mathcal{B}. \end{cases} \tag{14}$$

Finally by recalling the kinematic relations in Eq. (1), we can write

$$\begin{cases} u_{\mathrm{a}}' = \varepsilon_{\mathrm{a}}, & \text{in } \mathcal{B}, \\ u_{\mathrm{m}}' = \varepsilon_{\mathrm{m}}, & \text{in } \mathcal{B}, \\ \varepsilon_{\mathrm{a}}' = -h_{\mathrm{n}}(\varepsilon_{\mathrm{a}} - \varepsilon_{\mathrm{m}}) + h_{\mathrm{r}}(u_{\mathrm{a}} - u_{\mathrm{m}}), & \text{in } \mathcal{B}, \\ \varepsilon_{\mathrm{m}}' = \dfrac{h_{\mathrm{n}}}{h}(\varepsilon_{\mathrm{a}} - \varepsilon_{\mathrm{m}}) - \dfrac{h_{\mathrm{r}}}{h}(u_{\mathrm{a}} - u_{\mathrm{m}}), & \text{in } \mathcal{B}. \end{cases} \tag{15}$$

Equation (15) shows that in the considered case, the balance equations governing the deformation of the adhesive complex under study become a system of first-order, linear ODEs in space that can be analyzed with the standard tools used to study systems of first-order, linear ODEs in time. In this respect, we refer to Remark 1 for some details on this topic. Consequently, given the linearity of Eq. (15) with respect to the array of unknowns $\eta = [u_{\mathrm{a}}, u_{\mathrm{m}}, \varepsilon_{\mathrm{a}}, \varepsilon_{\mathrm{m}}]^{\mathrm{T}}$, also referred to as *state variable*, we can introduce the matrix A as

$$\mathsf{A} = \begin{bmatrix} 0 & 0 & 1 & 0 \\ 0 & 0 & 0 & 1 \\ h_{\mathrm{r}} & -h_{\mathrm{r}} & -h_{\mathrm{n}} & h_{\mathrm{n}} \\ -\dfrac{h_{\mathrm{r}}}{h} & \dfrac{h_{\mathrm{r}}}{h} & \dfrac{h_{\mathrm{n}}}{h} & -\dfrac{h_{\mathrm{n}}}{h} \end{bmatrix}, \tag{16}$$

so that the system of Eq. (15) can be recast as

$$\begin{bmatrix} u_{\mathrm{a}}' \\ u_{\mathrm{m}}' \\ \varepsilon_{\mathrm{a}}' \\ \varepsilon_{\mathrm{m}}' \end{bmatrix} = \mathsf{A} \begin{bmatrix} u_{\mathrm{a}} \\ u_{\mathrm{m}} \\ \varepsilon_{\mathrm{a}} \\ \varepsilon_{\mathrm{m}} \end{bmatrix} \qquad \text{in } \mathcal{B}, \tag{17}$$

or, briefly, as

$$\boldsymbol{\eta}' = \mathsf{A}\eta, \qquad \text{in } \mathcal{B}. \tag{18}$$

For the sake of completeness and for their use within the work, we study the geometric and spectral properties of the matrix A in Appendix A.

Remark 1. (*Space as order parameter for differential problems*) As reported above, we cast the problem of point-wise equilibrium in Eq. (15) into a system of first-order, linear ODEs in space as in Eq. (18). This reformulation is enabled by the linearity of the kinematic and constitutive relations in Eqs. (1) and (4), as well as the form of the elastic and non-elastic forces in Eqs. (6) and (9). In this respect, since we consider a rate independent problem of deformation, the natural order parameter is space only and is represented by the (spatial) variable $x \in \bar{\mathcal{B}}$. Although the mathematical formalism employed here follows the one typically used when time is the order parameter, it is important to emphasize the conceptual distinction

of the two physical scenarios. In our work, the problem is static: we are concerned in computing the deformed configuration of the adhesive system once body forces and boundary loads are applied[3]. In contrast, when temporal evolution is studied, we are interested in the system's final state, i.e., the state reached at the final instant of observation, as a consequence of the applied forces and the considered initial conditions. Accordingly, in the static case, the state space consists of displacement and its spatial derivative (displacement/deformation), whereas, in the dynamic case, it consists of displacement and its temporal derivative (displacement/velocity). In the remainder of the manuscript, whenever necessary, we will clarify how definitions and/or theorems that arise for dynamical systems are adapted to a problem of linear elastic deformation, represented by the first-order, linear system of ODEs in space as in Eq. (15).

Boundary conditions. For the scopes of our work, we select boundary conditions of the type

$$u_{\mathrm{a}}(0) = u_{\mathrm{a}0}, \qquad \sigma_{\mathrm{a}}(0) = \sigma_{\mathrm{a}0}, \tag{19a}$$

$$u_{\mathrm{m}}(0) = u_{\mathrm{m}0}, \qquad \sigma_{\mathrm{m}}(0) = \sigma_{\mathrm{m}0}, \tag{19b}$$

which, by virtue of Eq. (4), reformulate as

$$u_{\mathrm{a}}(0) = u_{\mathrm{a}0}, \qquad \varepsilon_{\mathrm{a}}(0) = \varepsilon_{\mathrm{a}0}, \tag{20a}$$

$$u_{\mathrm{m}}(0) = u_{\mathrm{m}0}, \qquad \varepsilon_{\mathrm{m}}(0) = \varepsilon_{\mathrm{m}0}. \tag{20b}$$

where we set $\varepsilon_{\mathrm{a}0} = \sigma_{\mathrm{a}0}/k_{\mathrm{a}}$ and $\varepsilon_{\mathrm{m}0} = \sigma_{\mathrm{m}0}/k_{\mathrm{m}}$. Although for dynamical systems it is natural to fix the value of the displacement and of its velocity at the origin (left end) of the (time) interval of observation (initial conditions), this is not the case of deformation. In fact, we cannot prescribe both displacement and deformation (or traction, because of linearity) on the same end-point of $\mathcal{B}$. On the other hand, due to the uniqueness of the solution, as proved in Appendix A, knowing the value of the deformation at $x = L$, one can uniquely compute its value at $x = 0$. For this reason, the choice of the boundary conditions in Eqs. (20a) and (20b) is then motivated.

2.3. A variational approach

In closing this section, we discuss a variational setting for the problem of adhesion considered in our work and, in particular, develop a modeling procedure based on the extended Hamilton variational principle [20] to also study how the non-elastic contribution $f^{(\mathrm{an})}$ breaks spatial symmetries. We anticipate that this approach will be also used in the forthcoming parts of the work to deduce the role of external forces acting on the adhesive system.

In the language of [20], we say that a generalized force F_α, with $\alpha \in \{\mathrm{a}, \mathrm{m}\}$, is said to be monogenic with respect to u_α, if there exists a generalized potential function $\mathcal{U} = \hat{\mathcal{U}}(u_{\mathrm{a}}, u'_{\mathrm{a}}, u_{\mathrm{m}}, u'_{\mathrm{m}}, x)$ such that

$$F_\alpha = \frac{\partial \hat{\mathcal{U}}}{\partial u_\alpha} - \frac{\mathrm{d}}{\mathrm{d}x}\left(\frac{\partial \hat{\mathcal{U}}}{\partial u'_\alpha}\right). \tag{21}$$

Otherwise, if Eq. (21) is not valid, we define F_α as polygenic generalized force [20]. We finally note that we use the terminology "generalized" since we consider Eq. (21) as a generalization of the standard definition of integrability, given in terms of a potential function depending on displacement only and a force is obtained by deriving such potential with respect to displacement. Let us introduce the Lagrangian density function $\mathcal{L} = \hat{\mathcal{L}}(u_{\mathrm{a}}, u_{\mathrm{m}}, u'_{\mathrm{a}}, u'_{\mathrm{m}})$ defined as the sum of the opposite of the strain energy function ψ in Eq. (3) and the potential U in Eq. (7), so that $\mathcal{L} = -\psi + U$ and

$$\mathcal{L} = \hat{\mathcal{L}}(u_{\mathrm{a}}, u_{\mathrm{m}}, u'_{\mathrm{a}}, u'_{\mathrm{m}}) = -\frac{1}{2}k_{\mathrm{a}}(u'_{\mathrm{a}})^2 - \frac{1}{2}k_{\mathrm{m}}(u'_{\mathrm{m}})^2 - \frac{k_{\mathrm{r}}}{2d_{\mathrm{r}}}(u_{\mathrm{a}} - u_m\mathrm{m})^2. \tag{22}$$

[3] Actually, we also study the case of external forces acting on the adhesive system, as done in Sect. 2.

We remark that $\mathcal{L}$, together with the axial deformation of the fibers, also accounts for the elastic force $f^{(\mathrm{el})}$ that is exchanged through the adhesive layer. In fact, such a force is *monogenic*, since it can be obtained as the derivative of U with respect to displacement as in Eq. (8). For what concerns the force term $f^{(\mathrm{an})}$ that describes the occurrence of non-elastic interactions between the top and the bottom fibers, it is not included in the definition of $\mathcal{L}$ in Eq. (22) because it is *polygenic*, whereas it is defined as the derivative of the Rayleigh-type function R in Eq. (10) with respect to axial deformation, as reported in Eq. (11). Accordingly, the Euler–Lagrange equations associated to the Lagrangian density function $\mathcal{L}$ in Eq. (22) are given by

$$\left(\frac{\partial \hat{\mathcal{L}}}{\partial u'_{\mathrm{a}}}\right)' - \frac{\partial \hat{\mathcal{L}}}{\partial u_{\mathrm{a}}} = -\frac{\partial R}{\partial u'_{\mathrm{a}}}, \qquad \text{in } \mathcal{B}, \tag{23a}$$

$$\left(\frac{\partial \hat{\mathcal{L}}}{\partial u'_{\mathrm{m}}}\right)' - \frac{\partial \hat{\mathcal{L}}}{\partial u_{\mathrm{m}}} = -\frac{\partial R}{\partial u'_{\mathrm{m}}}, \qquad \text{in } \mathcal{B}, \tag{23b}$$

leading, after some calculations, to Eq. (12) or, equivalently, to Eq. (14), if $\mathcal{L}$ is normalized with respect to k_{a}. We finally note that if we introduce the Jacobi, or mechanical, energy of the system, defined as

$$\begin{aligned}\mathcal{E} =& \hat{\mathcal{E}}(u_{\mathrm{a}}, u_{\mathrm{m}}, u'_{\mathrm{a}}, u'_{\mathrm{m}}) \\ =& \left[\frac{\partial \hat{\mathcal{L}}}{\partial u'_{\mathrm{a}}} \circ (u_{\mathrm{a}}, u_{\mathrm{m}}, u'_{\mathrm{a}}, u'_{\mathrm{m}})\right] u'_{\mathrm{a}} + \left[\frac{\partial \hat{\mathcal{L}}}{\partial u'_{\mathrm{m}}} \circ (u_{\mathrm{a}}, u_{\mathrm{m}}, u'_{\mathrm{a}}, u'_{\mathrm{m}})\right] u'_{\mathrm{m}} - \mathcal{L} \circ (u_{\mathrm{a}}, u_{\mathrm{m}}, u'_{\mathrm{a}}, u'_{\mathrm{m}}) \\ =& -\frac{1}{2} k_{\mathrm{a}} (u'_{\mathrm{a}})^2 - \frac{1}{2} k_{\mathrm{m}} (u'_{\mathrm{m}})^2 + \frac{k_{\mathrm{r}}}{2 d_{\mathrm{r}}} (u_{\mathrm{a}} - u_m)^2,\end{aligned} \tag{24}$$

its space derivative along the solution of Eq. (12) is computed as

$$\begin{aligned}\mathcal{E}' =& -k_{\mathrm{a}} u'_{\mathrm{a}} u''_{\mathrm{a}} - k_{\mathrm{m}} u'_{\mathrm{m}} u''_{\mathrm{m}} + \frac{k_{\mathrm{r}}}{d_{\mathrm{r}}} (u_{\mathrm{a}} - u_{\mathrm{m}})(u_{\mathrm{a}} - u_m \mathrm{m})' \\ =& -\left[k_{\mathrm{a}} u''_{\mathrm{a}} - \frac{k_{\mathrm{r}}}{d_{\mathrm{r}}} (u_{\mathrm{a}} - u_m \mathrm{m})\right] u'_{\mathrm{a}} - \left[k_{\mathrm{m}} u''_{\mathrm{m}} + \frac{k_{\mathrm{r}}}{d_{\mathrm{r}}} (u_{\mathrm{a}} - u_m \mathrm{m})\right] u'_{\mathrm{m}} \\ =& \frac{k_{\mathrm{n}}}{d_{\mathrm{r}}} (u'_{\mathrm{a}} - u'_m \mathrm{m})^2 \\ =& -2R,\end{aligned} \tag{25}$$

where we used the definition of the Rayleigh-like function in Eq. (10). In particular, the result reported in Eq. (25) means that the mechanical energy $\mathcal{E}$ of the adhesive system is not a first integral and, thus, is not conserved (in space). This implies that the symmetry related to the conservation of $\mathcal{E}$ is not valid, or broken, because of the presence of the non-elastic force $f^{(\mathrm{an})}$, discussed as polygenic. In conclusion, we remark that such loss of symmetry occurs even though the fibers and the adhesive layer are homogeneous, requiring $\hat{\mathcal{L}}$ to be independent on material points. In fact, also in the absence of material inhomogeneities, polygenic forces supply symmetry breaking [20].

3. The role of external forces

We discuss the effect of *external* agencies acting on the adhesive system under study with the wording *external* relating to all the (mechanical and non-mechanical) force-like interactions exchanged between the system and the external environment. We denote by $f_{\mathrm{a}}^{(\mathrm{ext})}$ and $f_{\mathrm{m}}^{(\mathrm{ext})}$ the family of such external forces[4] operating on the top and the bottom fiber, so that the point-wise system's equilibrium in Eqs.

[4] In fact, forces per unit of length and, similarly to $f^{(\mathrm{el})}$ and $f^{(\mathrm{an})}$, should be taken as body forces.

(26a) and (26b) is written in the form

$$\frac{\mathrm{d}\sigma_{\mathrm{a}}}{\mathrm{d}x} + f_{\mathrm{a}}^{(\mathrm{el})} + f_{\mathrm{a}}^{(\mathrm{an})} + f_{\mathrm{a}}^{(\mathrm{ext})} = 0, \qquad \text{in } \mathcal{B}, \tag{26a}$$

$$\frac{\mathrm{d}\sigma_{\mathrm{m}}}{\mathrm{d}x} + f_{\mathrm{m}}^{(\mathrm{el})} + f_{\mathrm{m}}^{(\mathrm{an})} + f_{\mathrm{m}}^{(\mathrm{ext})} = 0, \qquad \text{in } \mathcal{B}. \tag{26b}$$

also in light of Eq. (5). Accordingly, the extended Hamilton principle formulated in Eqs. (23a) and (23b) becomes

$$\left(\frac{\partial \hat{\mathcal{L}}}{\partial u_{\mathrm{a}}'}\right)' - \frac{\partial \hat{\mathcal{L}}}{\partial u_{\mathrm{a}}} = \frac{\partial R}{\partial u_{\mathrm{a}}'} + f_{\mathrm{a}}^{(\mathrm{ext})}, \qquad \text{in } \mathcal{B}, \tag{27a}$$

$$\left(\frac{\partial \hat{\mathcal{L}}}{\partial u_{\mathrm{m}}'}\right)' - \frac{\partial \hat{\mathcal{L}}}{\partial u_{\mathrm{m}}} = \frac{\partial R}{\partial u_{\mathrm{m}}'} + f_{\mathrm{m}}^{(\mathrm{ext})}, \qquad \text{in } \mathcal{B}, \tag{27b}$$

since both $f_{\mathrm{a}}^{(\mathrm{an})}$ and $f_{\mathrm{m}}^{(\mathrm{an})}$ are recognized as polygenic. In particular, they contribute to the non-spatial homogeneity of the Jacobi energy $\mathcal{E}$ in Eq. (24) as

$$\mathcal{E}' = -2R + \left[f_{\mathrm{a}}^{(\mathrm{ext})} u_{\mathrm{a}}' + f_{\mathrm{m}}^{(\mathrm{ext})} u_{\mathrm{m}}'\right]. \tag{28}$$

At this stage, it is important to discuss the way in which the external forces $f_{\mathrm{a}}^{(\mathrm{ext})}$ and $f_{\mathrm{m}}^{(\mathrm{ext})}$ should be selected. Following the modeling analysis proposed in [11], we consider two different strategies, named *a priori* and *a posteriori* controllability, hereafter discussed in detail.

***A priori* controllability.** Within such an approach, we require to give in advance the functional expression of both $f_{\mathrm{a}}^{(\mathrm{ext})}$ and $f_{\mathrm{m}}^{(\mathrm{ext})}$ in terms of the kinematic descriptors of our theory and, possibly, of the modeling parameters describing (mechanical or not) interactions with the external environment, denoted by ω. In this case, we set

$$f_{\alpha}^{(\mathrm{ext})} = \hat{f}_{\alpha}^{(\mathrm{ext})}(u_{\mathrm{a}}, u_{\mathrm{a}}', u_{\mathrm{m}}, u_{\mathrm{m}}', \omega, x), \quad \alpha \in \{\mathrm{a}, \mathrm{m}\}, \tag{29}$$

with ω being whether constant or depending on material points and with the expression of $\hat{f}_{\alpha}^{(\mathrm{ext})}$ chosen according to experiments or to phenomenological laws, with the scope of collecting pieces of information on the influence of external stimuli on the elastic deformation of the whole adhesive system. We note that although in the series of works [16,17] the wording *a priori* leads to the definition of a constrained (non-holonomic and rheonomic) problem, this is not the case in our work, since we do not prescribe any kinematic restriction on the state variable η, but we discuss the way in which the external forces $f_{\alpha}^{(\mathrm{ext})}$ should be assigned [11].

***A posteriori* controllability.** In this case, the form of the external forces $f_{\mathrm{a}}^{(\mathrm{ext})}$ and $f_{\mathrm{m}}^{(\mathrm{ext})}$ is not given at the beginning, but computed as a consequence of the overall (history of) deformation of the adhesive system. In particular, $f_{\mathrm{a}}^{(\mathrm{ext})}$ and $f_{\mathrm{m}}^{(\mathrm{ext})}$ are taken as functions of space and determined in such a way that the system reaches a prescribed placement. Accordingly, both $f_{\mathrm{a}}^{(\mathrm{ext})}$ and $f_{\mathrm{m}}^{(\mathrm{ext})}$ inherit the capability of driving the system's deformation toward a chosen state and, for this reason, are called *control functions*.

We remark that the difference between the two approaches is methodological, relying on the determination of the external forces and on their influence on the system's overall mechanical behavior: in the first case, the scope is to adhere to experimental evidences or to fit specific phenomenologies, while, in the second case, we device a suitable control problem. In both cases, the introduction of external forces is meant to unfold the interplay between the system's deformation and physical factors (of mechanical and/or non-mechanical type) coming from the external environment. It is worth mentioning that the literature offers different examples of modeling approaches accounting for the effect of external generalized forces. For instance, we mention [15], where the term "irreversible" refers to external momentum-like and

flux-like quantities acting on a growing system. Similarly, in [16,17], the terminology "non-conventional" collects non-mechanical actions describing external, (non-)mechanical agencies (chemo-mechanical coupling with nutrient factors flowing in the surrounding environment) influencing the volumetric growth of a hyperelastic medium, as previously discussed in [12].

3.1. *A posteriori* controllability: deformation as a control problem

From here on, we adopt the point of view of the *a posteriori* controllability and reformulate the equilibrium of the adhesive system subjected to external forces as a control problem. Accordingly, although the prescription of $f_{\mathrm{a}}^{(\mathrm{ext})}$ and $f_{\mathrm{m}}^{(\mathrm{ext})}$ could be crucial for a complete description of the adhesive system's deformation, also in relation with the external factors represented by ω, we do not claim any specific shape for them as functions of the state variable η, of the external factors ω and on material points. Instead, we interpret both $f_{\mathrm{a}}^{(\mathrm{ext})}$ and $f_{\mathrm{m}}^{(\mathrm{ext})}$ as the forces necessary to drive the deformation of the considered adhesive system toward a target placement. In this sense, we propose an *open loop* control-like approach [18] by virtue of which we study deformation as a space-dependent transformation of the reference placement into a prescribed one operated by suitable control functions.

We denote by $v_{\mathrm{a}}, v_{\mathrm{m}} : \mathcal{B} \to \mathbb{R}$ two control functions, having the physical unit of a displacement, and we define $f_{\mathrm{a}}^{(\mathrm{ext})}$ and $f_{\mathrm{m}}^{(\mathrm{ext})}$ as

$$f_{\mathrm{a}}^{(\mathrm{ext})} = \frac{k_{\mathrm{a}}^{(\mathrm{c})}}{d_{\mathrm{r}}} v_{\mathrm{a}}, \quad f_{\mathrm{m}}^{(\mathrm{ext})} = \frac{k_{\mathrm{m}}^{(\mathrm{c})}}{d_{\mathrm{r}}} v_{\mathrm{m}}, \tag{30}$$

where $k_{\mathrm{a}}^{(\mathrm{c})}$ and $k_{\mathrm{m}}^{(\mathrm{c})}$ are constant in space and, analogously to k_{r}, represent a force over length. By using Eqs. (4), (6) and (9) in Eqs. (26a) and (26b), in conjunction with Eq. (30), the field equations governing the equilibrium of the adhesive system under the action of the control functions v_{a} and v_{m} read

$$\begin{cases} (k_{\mathrm{a}} u_{\mathrm{a}}')' + \dfrac{k_{\mathrm{n}}}{d_{\mathrm{r}}}(u_{\mathrm{a}}' - u_{\mathrm{m}}') - \dfrac{k_{\mathrm{r}}}{d_{\mathrm{r}}}(u_{\mathrm{a}} - u_{\mathrm{m}}) + \dfrac{k_{\mathrm{a}}^{(\mathrm{c})}}{d_{\mathrm{r}}} v_{\mathrm{a}} = 0, & \text{in } \mathcal{B}, \\ (k_{\mathrm{m}} u_{\mathrm{m}}')' - \dfrac{k_{\mathrm{n}}}{d_{\mathrm{r}}}(u_{\mathrm{a}}' - u_{\mathrm{m}}') + \dfrac{k_{\mathrm{r}}}{d_{\mathrm{r}}}(u_{\mathrm{a}} - u_{\mathrm{m}}) + \dfrac{k_{\mathrm{m}}^{(\mathrm{c})}}{d_{\mathrm{r}}} v_{\mathrm{m}} = 0, & \text{in } \mathcal{B}, \end{cases} \tag{31}$$

Finally, we introduce the notation

$$h_{\mathrm{a}}^{(\mathrm{c})} = \frac{k_{\mathrm{a}}^{(\mathrm{c})}}{k_{\mathrm{a}} d_{\mathrm{r}}}, \quad h_{\mathrm{m}}^{(\mathrm{c})} = \frac{k_{\mathrm{m}}^{(\mathrm{c})}}{k_{\mathrm{a}} d_{\mathrm{r}}}, \tag{32}$$

where $h_{\mathrm{a}}^{(\mathrm{c})}$ and $h_{\mathrm{m}}^{(\mathrm{c})}$ have the dimension of the inverse of an area (analogously to h_{r}), so that Eq. (31) admits the following normalized version (with respect to k_{a})

$$\begin{cases} u_{\mathrm{a}}'' + h_{\mathrm{n}}(u_{\mathrm{a}}' - u_{\mathrm{m}}') - h_{\mathrm{r}}(u_{\mathrm{a}} - u_{\mathrm{m}}) + h_{\mathrm{a}}^{(\mathrm{c})} v_{\mathrm{a}} = 0, & \text{in } \mathcal{B}, \\ u_{\mathrm{m}}'' - \dfrac{h_{\mathrm{n}}}{h}(u_{\mathrm{a}}' - u_{\mathrm{m}}') + \dfrac{h_{\mathrm{r}}}{h}(u_{\mathrm{a}} - u_{\mathrm{m}}) + \dfrac{h_{\mathrm{m}}^{(\mathrm{c})}}{h} v_{\mathrm{m}} = 0, & \text{in } \mathcal{B}. \end{cases} \tag{33}$$

and its counterpart as a system of linear ODEs

$$\begin{cases} u'_{\mathrm{a}} = \varepsilon_{\mathrm{a}}, & \text{in } \mathcal{B}, \\ u'_{\mathrm{m}} = \varepsilon_{\mathrm{m}}, & \text{in } \mathcal{B}, \\ \varepsilon'_{\mathrm{a}} = -h_{\mathrm{n}}(\varepsilon_{\mathrm{a}} - \varepsilon_{\mathrm{m}}) + h_{\mathrm{r}}(u_{\mathrm{a}} - u_{\mathrm{m}}) - h_{\mathrm{a}}^{(\mathrm{c})} v_{\mathrm{a}}, & \text{in } \mathcal{B}, \\ \varepsilon'_{\mathrm{m}} = \dfrac{h_{\mathrm{n}}}{h}(\varepsilon_{\mathrm{a}} - \varepsilon_{\mathrm{m}}) - \dfrac{h_{\mathrm{r}}}{h}(u_{\mathrm{a}} - u_{\mathrm{m}}) - \dfrac{h_{\mathrm{m}}^{(\mathrm{c})}}{h} v_{\mathrm{m}}, & \text{in } \mathcal{B}. \end{cases} \tag{34}$$

In conclusion, we introduce the matrix $\mathsf{B} \in \mathbb{R}^{4x\times 2}$, defined as

$$\mathsf{B} = \begin{bmatrix} 0 & 0 \\ 0 & 0 \\ -h_{\mathrm{a}}^{(\mathrm{c})} & 0 \\ 0 & -h_{\mathrm{m}}^{(\mathrm{c})}/h \end{bmatrix}, \tag{35}$$

and put Eq. (34) in the form of a system of linear ODEs

$$\boldsymbol{\eta}' = \mathsf{A}\eta + \mathsf{B}v, \qquad \text{in } \mathcal{B}, \tag{36}$$

where $v = [v_{\mathrm{a}}, v_{\mathrm{m}}]^{\mathrm{T}}$ is the bi-dimensional array of controls. Before going further, two remarks are in order. Firstly, the point-wise equilibrium of the adhesive system under the influence of external forces in Eq. (34), cast in the form of Eq. (36), implies that the *a posteriori* controllability is studied as controllability of the system of linear ODEs $\boldsymbol{\eta}' = \mathsf{A}\eta + \mathsf{B}v$. Secondly, Eqs. (35) and (36) express intrinsic *underactuation* [2], since the number of controls is less than the state variables. In fact, by introducing the external forces in the equilibrium equations as in Sect. 3.1, controls act only on deformations and not on displacements.

4. Geometric control theory: a brief review

We summarize the main results of Geometric Control Theory as applied to systems of first-order, linear ODEs. In particular, we provide the key definitions, theorems and properties necessary for a complete *control* analysis of the adhesive system under study, whose mechanical equilibrium is represented as a linear space control problem in Eq. (34), with the space variable $x \in \bar{\mathcal{B}}$ taken as the order parameter in our framework (we refer to Remark 1).

Having in mind the control scenario, we use the space-dependent control functions v_{a} and v_{m} to drive the system, finding in the reference placement $\mathcal{B}$, toward a deformed placement with a desired boundary value in $x = L$, knowing the boundary state in $x = 0$. The main technical tools of Geometric Control Theory are applicable in a straightforward way also in this context and enlisted in the rest of the present section, together with the notation used hereafter.

4.1. General definitions

A control system in space, in its general formulation, is a mathematical model designed to pilot the deformation and the mechanical response of a structural system through the application of suitable space-dependent control functions that, assigned the system's reference state (displacement and traction at $x = 0$, in our work), steer it to *reach* a target specified state (at $x = L$, for our one-dimensional problem).

Definition 1. (Control system in space [6]) A control system in space is represented as a system of first-order ODEs that, on its normal form, is written as

$$\boldsymbol{\eta}' = \boldsymbol{\mathcal{F}}(\eta, v). \tag{37}$$

In Eq. (37), and given $N, M \in \mathbb{N}$, $\eta \in \mathcal{Q} \subset \mathbb{R}^N$ collects the local coordinates of a smooth, open manifold $\mathcal{Q}$, the state space, and is meant to display the state variables of the system at hand, $v : [0, L] \to \mathcal{V} \subset \mathbb{R}^M$, is an array of measurable control functions belonging to $\mathcal{V}$, being the latter an open subset of $\mathbb{R}^M$, referred to as the set of admissible controls, while $\boldsymbol{\mathcal{F}} : \mathcal{Q} \times \mathcal{V} \to \mathbb{R}^N$ is a (sufficiently regular) vector field.

Before going further, we remark that the functional expression of $\boldsymbol{\mathcal{F}}$, representing the relationship between the controls and state variables, can be nonlinear, so that the control system in Eq. (37), consisting of nonlinear differential equations of the first order, is said to be nonlinear.

From now on, we restrict ourselves to *linear control* systems, i.e., control systems with $\boldsymbol{\mathcal{F}}$ to be linear with respect to both η and v and, for the scopes of our work, we take

$$\boldsymbol{\mathcal{F}}(\eta, v) = \mathsf{A}\eta + \mathsf{B}v, \tag{38}$$

where $\mathsf{A} \in \mathbb{R}^{N\times N}$ and $\mathsf{B} \in \mathbb{R}^{N\times M}$. We now give the definition of solution of a linear control system. To this end, we set $\mathcal{Q} \equiv \mathbb{R}^N$ and $\mathcal{V} \equiv \mathbb{R}^M$,

Definition 2. (Solution [6]) Given $v \in L^\infty([0, L], \mathbb{R}^M)$, a *solution* of the (space) linear control system $\boldsymbol{\eta}' = \mathsf{A}\eta + \mathsf{B}v$, along with the boundary condition $\eta(0) = \eta_0 \in \mathbb{R}^N$, is a function $\eta : [0, L] \to \mathbb{R}^N$, with

$$\eta \in C^0([0, L]; \mathbb{R}^N), \tag{39}$$

and admitting the following integral expression

$$\bar{\eta}(x) = \eta_0 + \int_0^x [\mathsf{A}\eta(s) + \mathsf{B}v(s)]\, \mathrm{d}s, \quad x \in [0, L]. \tag{40}$$

As a next step, we consider the crucial notion of space *controllability*, which pertains to the capability of a (one-dimensional) system to be driven toward a placement corresponding to *a* boundary condition at $x = 0$ and *any* specified boundary condition at $x = L$ under the action of control inputs. The latter, in any case, should belong to a certain functional space. It is important to recall that prescribing both the boundary condition at $x = 0$ and at $x = L$ is not in contradiction with that reported at the end of Sect. 2.2, since, as long as the control is not identified, the solution is not unique. Once the control function is computed, the solution of Eq. (38) becomes unique and given by Eq. (40). By following Geometric Control Theory, and with reference to linear systems only, we provide the following definition.

Definition 3. (Space controllability [6]) The linear control system of Eq. (38) is said to be controllable in space if, for any η_0, $\eta_L \in \mathbb{R}^N$, there exists a control function $v \in L^\infty([0, L], \mathbb{R}^M)$ such that $\eta(0) = \eta_0$ and $\eta(L) = \eta_L$.

In other words, space controllability essentially means that a system can be *driven* or *controlled* to pass from the reference placement $\mathcal{B}$ to any deformed placement with fixed η_0 and target boundary condition η_L. The array of controls v can been seen as the external input or action required to accomplish this task. Furthermore, we remark that both in Definition 2 and 3, we select the control function $v \in L^\infty([0, L], \mathbb{R}^M)$, although it is possible to alternatively set $v \in L^1([0, L], \mathbb{R}^M)$ or $v \in L^2([0, L], \mathbb{R}^M)$. Following [6], this choice is motivated since $L^\infty([0, L], \mathbb{R}^M)$ is the natural ambient space to discuss controllability of nonlinear systems and the properties of controllability for linear systems are not affected by the functional space to in which controls are defined.

For linear control systems as in Eq. (38), several criteria to prove their controllability are available in the literature (see, for instance [6] and references therein). Hereafter, we employ the well-known *Kalman Rank condition*, representing a necessary and sufficient condition of controllability based on the algebraic properties of the two matrices A and B.

Theorem 1. *The linear control system* $\boldsymbol{\eta}' = \mathsf{A}\eta + \mathsf{B}v$ *is controllable in space with respect to the reference placement* $\mathcal{B} = [0, L]$ *if and only if*

$$\operatorname{span}\{\mathsf{A}^i\mathsf{B}v,\, v \in \mathbb{R}^M,\, i = \{0, \dots, N-1\}\} = \mathbb{R}^N. \tag{41}$$

Remark 2. Note that whatever $L_0 < L_1$ are, the linear control system $\boldsymbol{\eta}' = \mathsf{A}\eta + \mathsf{B}v$ is controllable in space on $[0, L]$ if and only if it is controllable in space on $[L_0, L_1]$.

Finally, after introducing the *controllability* or *Kalman matrix* C, defined as

$$\mathsf{C} = \left[\mathsf{B}v | \mathsf{A}\,\mathsf{B}v | \mathsf{A}^2\,\mathsf{B}v | \dots | \mathsf{A}^{n-1}\mathsf{B}v\right], \tag{42}$$

the linear control system $\boldsymbol{\eta}' = \mathsf{A}\eta + \mathsf{B}v$ is controllable if and only if the rank of the matrix C is maximum and, hence, equal to N.

4.2. Optimal control

In this section, we give the fundamental definitions and theorems regarding linear–quadratic Optimal Control Theory that we will employ in the subsequent sections. Consequently, once the problem of space controllability is discussed and solved, we study how to compute optimal trajectories for the adhesive system to pass from the reference placement $\mathcal{B}$ to a target one, driven by optimal control functions satisfying certain (optimality) criteria. It is trivial to note that a problem of linear–quadratic Optimal Control is strongly influenced by the chosen optimality conditions, as well as the geometric/structural properties of the matrices A and B [2,6,18,34]. Hereafter, also to answer all the purposes of the work, we focus on the problem of minimizing a cost function and discuss all the technical details and results in light of the Maximum Principle proposed by Pontryagin [34], suitably adapted to linear control systems of ODEs in space. We only recall that the Pontryagin Maximum Principle[5] consists in identifying the necessary conditions of optimality, without being, in general, sufficient [2,6,18,34], for achieving the optimal control driving the presence of constraints on the state variables and/or controls. A general overview of the Pontryagin Maximum Principle for linear systems is reported in Appendix B.

4.2.1. PMP for linear–quadratic problems. The minimizing functional reads

$$\min_{v(\cdot)} J(v) = \frac{1}{2}\Psi(\eta(L), L) + \frac{1}{2}\int_0^L \left[\eta(x)^\top \mathsf{Q}\,\eta(x) + v(x)^\top \mathsf{R}\,v(x)\right] \mathrm{d}x, \tag{43}$$

$$\text{subject to} \quad \boldsymbol{\eta}' = \mathsf{A}\eta + \mathsf{B}v, \qquad \eta(0) = \eta_0, \tag{44}$$

where the constant matrices $\mathsf{Q} \in \mathbb{R}^N$ and $\mathsf{R} \in \mathbb{R}^M$ are symmetric and positive definite. Then the Pontryagin's Hamiltonian function reads

$$\hat{H}(\eta, v, p) = p^\top(\mathsf{A}\eta + \mathsf{B}v) - \tfrac{1}{2}\left(\eta^\top \mathsf{Q}\,\eta + v^\top \mathsf{R}\,v\right).$$

The following necessary conditions hold for an optimal control v^* and its corresponding optimal trajectory η^*

$$\boldsymbol{\eta}^{*'} = \frac{\partial \hat{H}}{\partial p}(\eta^*, v^*, p) = \mathsf{A}\eta^* + \mathsf{B}v^*, \tag{45a}$$

$$\boldsymbol{p}' = -\frac{\partial \hat{H}}{\partial \eta}(\eta^*, v^*, p) = -\mathsf{A}^\top p + \mathsf{Q}\eta^*, \tag{45b}$$

[5] The principle was initially known as the Pontryagin Maximum Principle, and thus, its proof was based on maximizing an Hamiltonian function, the Pontryagin's Hamiltonian. Since it was later used in numerous minimization problems, it also became known as the Pontryagin Minimum Principle [34].

while the stationary condition of the Hamiltonian with respect to v leads to

$$v^* = \mathsf{R}^{-1}\mathsf{B}^\top p, \tag{46}$$

and the transversality conditions are the one in Eq. (87). We conclude this section by enunciating the following theorem that guarantees the existence of a unique solution for the optimization of a linear-quadratic problem.

Theorem 2. (Existence of an optimal solution [34]) *Assume that there exists a real scalar* $\alpha > 0$ *such that*

$$\forall v \in L^2([0,L],\mathbb{R}^m), \quad \int_0^L v^{\mathrm{T}}(x)\mathsf{R}v(x)\,dx \geq \alpha \int_0^L v^{\mathrm{T}}(x)v(x)\,ds.$$

Then there exists a unique minimizing solution for the linear quadratic optimal control problem in Eqs. (82a)–(82b).

Note that considering $v \in L^2([0,L],\mathbb{R}^M)$ is not in conflict with the fact that the controllability results in Sect. 4.1 are stated with $v \in L^\infty([0,L],\mathbb{R}^M)$, indeed, since we are on the compact set $[0,L]$, we naturally have $L^\infty([0,L],\mathbb{R}^M) \subset L^2([0,L],\mathbb{R}^M)$.

5. Controllability and optimal control for adhesion

We now apply the methods of Geometric Control Theory (see Sect. 4) to analyze the structural behavior of the considered adhesive system in response to external stimuli, with the latter modeled as control functions. In other words, we study what happens when controls in space are added to the equations of point-wise equilibrium, with the purpose to make the system reaching any desired state prescribed in $x = L$, even starting from an equilibrium point (in this sense, we refer to Appendix A.1). In what follows, we analyze different situations, framed in the general modeling approach previously developed.

In the considered problem, we have $N = 4$, since the problem of adhesion under study is represented by the four kinematic descriptors $u_\mathrm{a}, u_\mathrm{m}, \varepsilon_\mathrm{a}$ and ε_m, collected in the array $\eta = [u_\mathrm{a}, u_\mathrm{m}, \varepsilon_\mathrm{a}, \varepsilon_\mathrm{m}] \in \mathbb{R}^4$. Moreover, we take $M \leq 2 < N$, because the control functions are represented by the array $v = [v_\mathrm{a}, v_\mathrm{m}]^\mathrm{T}$ or by the single functions v_a or v_m if one of them is null. Finally, the matrix A is defined in Eq. (16) and the matrix B in Eq. (35). In particular, being both A and B expressed in terms of the space-independent material properties of the adhesive system, they are constant with respect to $x \in \mathcal{B}$.

5.1. Case of controlled top fiber

We start by considering the case in which only the external force $f_\mathrm{a}^{(\mathrm{ext})}$ acts on the adhesive system, with $f_\mathrm{m}^{(\mathrm{ext})} = 0$ taken to be absent and, thus, $v_\mathrm{m} = 0$. Accordingly we have that $M = 1$, the array of controls corresponds to v_a only and the matrix B in Eq. (35) reduces to

$$\mathsf{B}_\mathrm{a} = \begin{bmatrix} 0 \\ 0 \\ -h_\mathrm{a}^{(\mathrm{c})} \\ 0 \end{bmatrix}. \tag{47}$$

The final form of the control system, in this case, is given by

$$\begin{bmatrix} u_\mathrm{a}' \\ u_\mathrm{m}' \\ \varepsilon_\mathrm{a}' \\ \varepsilon_\mathrm{m}' \end{bmatrix} = \mathsf{A} \begin{bmatrix} u_\mathrm{a} \\ u_\mathrm{m} \\ \varepsilon_\mathrm{a} \\ \varepsilon_\mathrm{m} \end{bmatrix} + \begin{bmatrix} 0 \\ 0 \\ -h_\mathrm{a}^{(\mathrm{c})} \\ 0 \end{bmatrix} v_\mathrm{a}. \tag{48}$$

We remark that since v_a appears in the (normalized) equation of ε'_a only, we say that we are controlling the top fiber's deformation. To assess space controllability by testing the Kalman Rank condition, we compute the controllability matrix as $\mathsf{C}_\mathrm{a} = [\mathsf{B}_\mathrm{a}|\mathsf{A}\mathsf{B}_\mathrm{a}|\mathsf{A}^2\mathsf{B}_\mathrm{a}|\mathsf{A}^3\mathsf{B}_\mathrm{a}]$ (see Theorem 1 and Eq. (42)), where

$$\mathsf{A}\mathsf{B}_\mathrm{a} = \frac{h_\mathrm{a}^{(\mathrm{c})}}{h}\begin{bmatrix} -h \\ 0 \\ h_\mathrm{n} h \\ -h_\mathrm{n} \end{bmatrix}, \tag{49a}$$

$$\mathsf{A}^2\mathsf{B}_\mathrm{a} = \frac{h_\mathrm{a}^{(\mathrm{c})}}{h^2}\begin{bmatrix} h_\mathrm{n} h^2 \\ -h_\mathrm{n} h \\ -h\,(1+h)\,h_\mathrm{n}^2 - h_\mathrm{r} h^2 \\ (1+h)h_\mathrm{n}^2 + h h_\mathrm{r} \end{bmatrix}, \tag{49b}$$

$$\mathsf{A}^3\mathsf{B}_\mathrm{a} = \frac{h_\mathrm{a}^{(\mathrm{c})}}{h^3}\begin{bmatrix} -h^2\,(1+h)\,h_\mathrm{n}^2 - h_\mathrm{r} h^3 \\ h(1+h)h_\mathrm{n}^2 + h^2 h_\mathrm{r} \\ h(1+h)^2 h_\mathrm{n}^3 + 2h^2 h_\mathrm{r} h_\mathrm{n}(1+h) \\ -(1+h)h_\mathrm{n}[(1+h)h_\mathrm{n}^2 + 2h h_\mathrm{r}] \end{bmatrix}. \tag{49c}$$

Finally, we compute the determinant $\det\mathsf{C}_\mathrm{a} = -\left(h_\mathrm{a}^{(\mathrm{c})}\right)^4 h_\mathrm{r}^2/h^2 \neq 0$. Hence, the rank of C_a is maximum and, by virtue of Theorem 1, the system is controllable in space with an external force acting on the top fiber only.

5.2. Case of controlled bottom fiber

We here consider only the external force $f_\mathrm{m}^{(\mathrm{ext})}$ acting on the adhesive system and, in particular, we set $f_\mathrm{a}^{(\mathrm{ext})} = 0$ and $v_\mathrm{a} = 0$. Thus, the array of controls reduces to v_m solely and the matrix B (compare with Eq. (35)) becomes

$$\mathsf{B}_\mathrm{m} = \begin{bmatrix} 0 \\ 0 \\ 0 \\ -h_\mathrm{m}^{(\mathrm{c})}/h \end{bmatrix}. \tag{50}$$

Also in this case, we compute the controllability matrix as $\mathsf{C}_\mathrm{m} = [\mathsf{B}_\mathrm{m}|\mathsf{A}\mathsf{B}_\mathrm{m}|\mathsf{A}^2\mathsf{B}_\mathrm{m}|\mathsf{A}^3\mathsf{B}_\mathrm{m}]$ (we refer again to Theorem 1 and Eq. (42)), with

$$\mathsf{A}\mathsf{B}_\mathrm{m} = \frac{h_\mathrm{m}^{(\mathrm{c})}}{h^2}\begin{bmatrix} 0 \\ -h \\ -h_\mathrm{n} h \\ h_\mathrm{n} \end{bmatrix}, \tag{51a}$$

$$\mathsf{A}^2\mathsf{B}_\mathrm{m} = \frac{h_\mathrm{m}^{(\mathrm{c})}}{h^3}\begin{bmatrix} -h_\mathrm{n} h^2 \\ h_\mathrm{n} h \\ h\,(1+h)\,h_\mathrm{n}^2 + h_\mathrm{r} h^2 \\ -(1+h)h_\mathrm{n}^2 - h h_\mathrm{r} \end{bmatrix}, \tag{51b}$$

$$\mathsf{A}^3\mathsf{B}_\mathrm{m} = \frac{h_\mathrm{m}^{(\mathrm{c})}}{h^4}\begin{bmatrix} h^2\,(1+h)\,h_\mathrm{n}^2 + h_\mathrm{r}h^3 \\ -h(1+h)h_\mathrm{n}^2 - h^2h_\mathrm{r} \\ -h(1+h)^2h_\mathrm{n}^3 - 2h^2h_\mathrm{r}h_\mathrm{n}(1+h) \\ (1+h)h_\mathrm{n}[(1+h)h_\mathrm{n}^2 + 2hh_\mathrm{r}] \end{bmatrix}. \tag{51c}$$

Also in this case, the matrix C_m has maximum rank, since $\det\mathsf{C}_\mathrm{m} = \left(h_\mathrm{m}^{(\mathrm{c})}\right)^4 h_\mathrm{r}^2/h^4 \neq 0$ and, thus, the system is controllable in space with an external force acting on the bottom fiber only, by virtue of Theorem 1.

5.3. Case of controlled both fibers

We now consider the effect of both the external forces $f_\mathrm{a}^{(\mathrm{ext})}$ and $f_\mathrm{m}^{(\mathrm{ext})}$. In particular, the array of control functions is $v = [v_\mathrm{a}, v_\mathrm{m}]^\mathrm{T}$ and

$$\begin{bmatrix} u_\mathrm{a}' \\ u_\mathrm{m}' \\ \varepsilon_\mathrm{a}' \\ \varepsilon_\mathrm{m}' \end{bmatrix} = \mathsf{A}\begin{bmatrix} u_\mathrm{a} \\ u_\mathrm{m} \\ \varepsilon_\mathrm{a} \\ \varepsilon_\mathrm{m} \end{bmatrix} + \mathsf{B}\begin{bmatrix} v_\mathsf{a} \\ v_\mathrm{m} \end{bmatrix}. \tag{52}$$

In this case, once the controllability matrix C is computed, it is trivial to note that C has rank equal to four and the system is then controllable in light of Theorem 1. Consequently, we can speak of *underactuated control systems* [2], since controllability in space can be achieved with an array of control functions of dimension smaller than that of η. Heuristically, if the system is controllable with one function, it is for sure controllable with two functions.

5.4. Optimal control: relevant cases and simulations

Since we have verified the controllability of the adhesive system under the action of the external forces $f_\mathrm{a}^{(\mathrm{ext})}$ and $f_\mathrm{m}^{(\mathrm{ext})}$, we want to address some Linear-Quadratic optimal control problems which differ for the chosen functional to minimize. In particular, we focus on the case of controlled bottom fiber, with the only non-null control function being v_m.

We perform FEM-based numerical simulations of the optimal control of the adhesive system, and we impose suitable boundary conditions for the state variables at the left boundary of the system, by assigning $u_{\mathrm{a}0}$, $u_{\mathrm{m}0}$, $\varepsilon_{\mathrm{a}0}$ and $\varepsilon_{\mathrm{m}0}$. We remark that although we consider values of the material parameters by taking inspiration from focal adhesions (see [4,9] and Table 1), no specific application of our model is proposed in this work[6].

5.4.1. Minimal distance from a "target" state. We examine the case in which the cost functional minimizes the distance from a "target" state. Such functional is composed of a *running cost*, which is a weighted L^2-distance from the "target" state $\bar\eta = [\bar u_\mathrm{a}, \bar u_\mathrm{m}, \bar\varepsilon_\mathrm{a}, \bar\varepsilon_\mathrm{m}]^\mathrm{T}$ together with the L^2-norm of the control function v_m, so that we do reach a target state using a control with the smallest norm possible. Moreover, the target state is also present in the terminal cost function, since we penalize ending up at $\eta(L)$ instead of $\bar\eta$; thus, it represents also the desired terminal value of the system. Hence, the functional reads

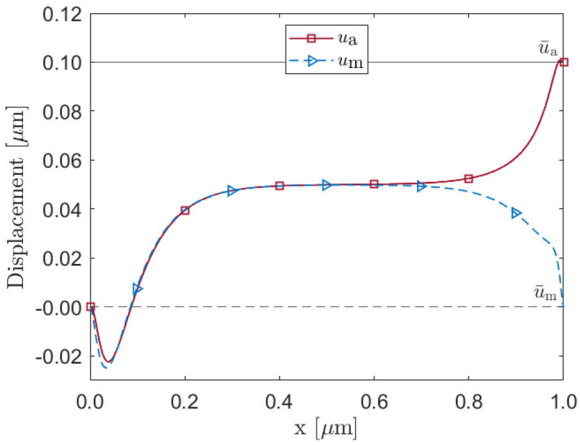
$$J(v) = \frac{1}{2}\mu_\Psi d_\mathrm{r}\left\{\zeta[u_\mathrm{a}(L) - \bar u_\mathrm{a}]^2 + \zeta[u_\mathrm{m}(L) - \bar u_\mathrm{m}]^2 + [\varepsilon_\mathrm{a}(L) - \bar\varepsilon_\mathrm{a}]^2 + h[\varepsilon_\mathrm{m}(L) - \bar\varepsilon_\mathrm{m}]^2\right\}$$

[6] Details on this topic are given in Sect. 6.

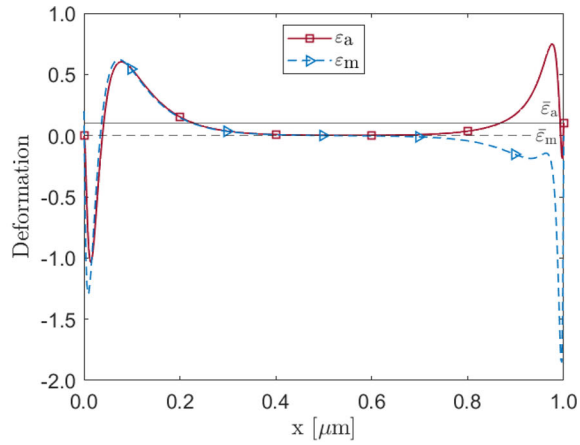
TABLE 1. Values of the material parameters used for the numerical simulations

Symbol	Numerical value	Unit of measure
L	1000.0	nm
k_{a}	100.0	pN
k_{m}	250.0	pN
k_{r}	30.0	pN/nm
k_{n}	2000.0	pN
d_{r}	200.0	nm
μ_{Ψ}	1000.0	−
ζ	$1/d_{\mathrm{r}}^2$	nm^{-2}
$k_{\mathrm{m}}^{(\mathrm{c})}$	312.5	pN/nm

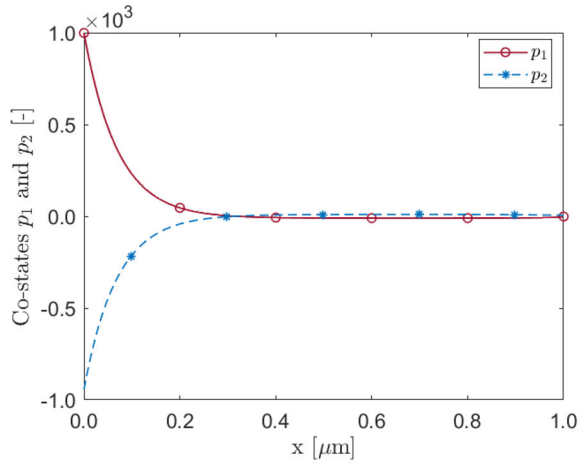
Most of the values have been taken from [4] and [9]. The adimensionalized parameter used in the simulations has been obtained by recurring to Eq. (13)



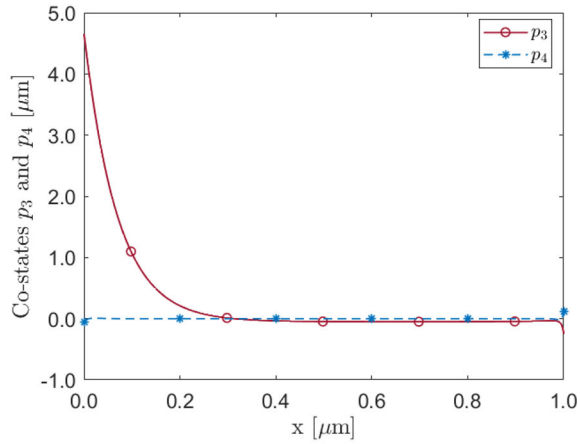
(A)
Spatial distribution of the displacements of the top and bottom fibers.



(B)
Spatial distribution of the deformations of the top and bottom fibers.



(C)
Spatial distribution of the co-states p_1 and p_2.

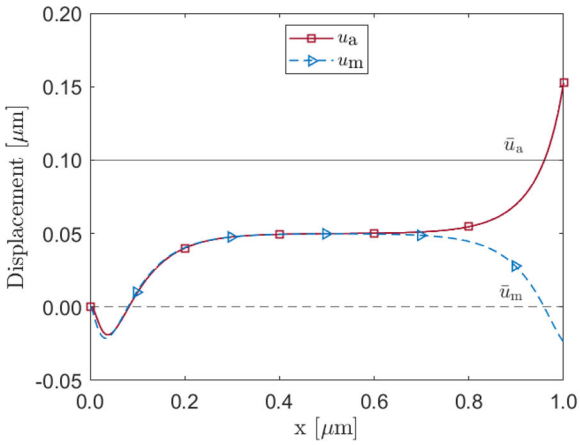


(D)
Spatial distribution of the co-states p_3 and p_4.

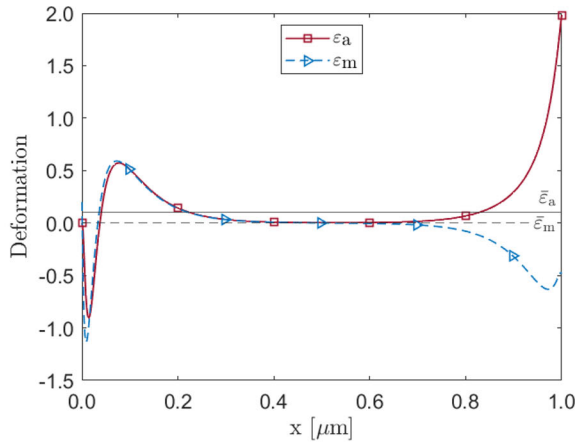
FIG. 2. State and co-state variables of the adhesive systems in the case of minimal distance from a target state and prescribed cost for running up at η (see Eq. (53))

$$+\frac{1}{2}\int_0^L \Big\{ h_r[u_a(x)-\bar{u}_a]^2+h_r[u_m(x)-\bar{u}_m]^2+[\varepsilon_a(x)-\bar{\varepsilon}_a]^2+h[\varepsilon_m(x)-\bar{\varepsilon}_m]^2+h_m^{(c)}v_m^2(x)\Big\}\mathrm{d}x$$

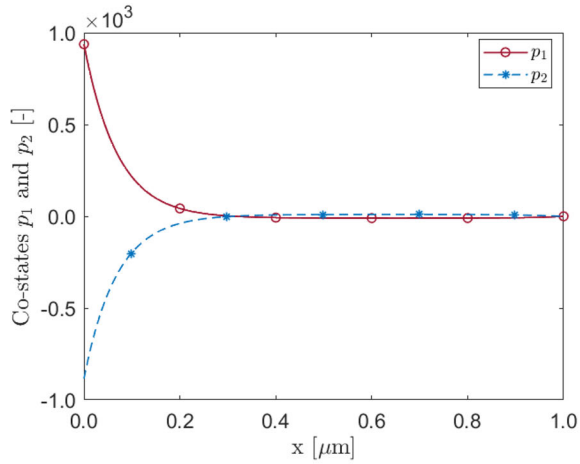
$$=\frac{1}{2}[\eta(L)-\bar{\eta}]^{\mathrm{T}}\mathsf{U}\,[\eta(L)-\bar{\eta}]+\frac{1}{2}\int_0^L \{[\eta(x)-\bar{\eta}]^{\mathrm{T}}\mathsf{Q}\,[\eta(x)-\bar{\eta}]+h_m^{(c)}v_m^2(x)\}\mathrm{d}x, \tag{53}$$



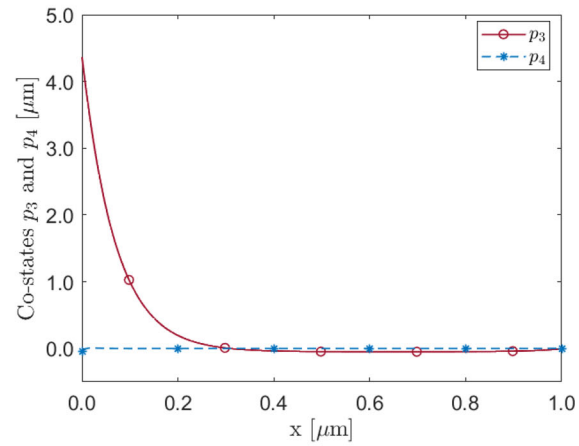
(A)
Spatial distribution of the displacements of the top and bottom fibers.



(B)
Spatial distribution of the deformations of the top and bottom fibers.



(C)
Spatial distribution of the co-states p_1 and p_2.



(D)
Spatial distribution of the co-states p_3 and p_4.

FIG. 3. State and co-state variables of the adhesive systems in the case of minimal distance from a target state when the cost for running up at η is null (see Eq. (53)), by setting $\mu_\psi = 0$)

where we introduced the constant parameters ζ (inverse of a square length) and μ_Ψ (non-dimensional), along with the matrices U and Q defined as

$$\mathsf{U} = \mu_\Psi d_r \begin{bmatrix} \zeta & 0 & 0 & 0 \\ 0 & \zeta & 0 & 0 \\ 0 & 0 & 1 & 0 \\ 0 & 0 & 0 & h \end{bmatrix}, \qquad \mathsf{Q} = \begin{bmatrix} h_r & 0 & 0 & 0 \\ 0 & h_r & 0 & 0 \\ 0 & 0 & 1 & 0 \\ 0 & 0 & 0 & h \end{bmatrix}. \tag{54}$$

The parameters ζ and μ_ψ play the role of *penalization parameters* that set the magnitude of the reaction forces imposed in the terminal state of the system via transversality conditions. It is important to notice that in the case under study, these constants are calibrated from the outset in a way that the reaction

forces are comparable with the elastic response originating from the mechanics of the system. The same approach is used for determining $h_{\mathrm{m}}^{(\mathrm{c})}$.

Remark 3. (*Cost functional affine in* η) In the case under study, the cost functional in Eq. (53) is not of the form specified in Eq. (43), since it is not a linear-quadratic problem in η. However, by introducing the auxiliary variable $\xi = \eta - \bar{\eta}$, the cost functional is quadratic in ξ and the equations of motion become $\xi' = \mathsf{A}\xi + \mathsf{B}v + \mathsf{A}\bar{\eta}$. However, per Remark 4.0.4 of Trélat [34], the results regarding the existence and uniqueness of an optimal solution and the PMP hold true nevertheless.

The application of PMP gives the following system of equations

$$\begin{cases} u_{\mathrm{a}}' = \varepsilon_{\mathrm{a}} \\ u_{\mathrm{m}}' = \varepsilon_{\mathrm{m}} \\ \varepsilon_{\mathrm{a}}' = -h_{\mathrm{n}}(\varepsilon_{\mathrm{a}} - \varepsilon_{\mathrm{m}}) + h_{\mathrm{r}}(u_{\mathrm{a}} - u_{\mathrm{m}}) \\ \varepsilon_{\mathrm{m}}' = \dfrac{h_{\mathrm{n}}}{h}(\varepsilon_{\mathrm{a}} - \varepsilon_{\mathrm{m}}) - \dfrac{h_{\mathrm{r}}}{h}(u_{\mathrm{a}} - u_{\mathrm{m}}) + \dfrac{h_{\mathrm{m}}^{(\mathrm{c})}}{h^2} p_4 \\ p_1' = h_{\mathrm{r}}(u_{\mathrm{a}} - \bar{u}_{\mathrm{a}}) - h_{\mathrm{r}} p_3 + \dfrac{h_{\mathrm{r}}}{h} p_4 \\ p_2' = h_{\mathrm{r}}(u_{\mathrm{m}} - \bar{u}_{\mathrm{m}}) + h_{\mathrm{r}} p_3 - \dfrac{h_{\mathrm{r}}}{h} p_4 \\ p_3' = (\varepsilon_{\mathrm{a}} - \bar{\varepsilon}_{\mathrm{a}}) - p_1 + h_{\mathrm{n}} p_3 - \dfrac{h_{\mathrm{n}}}{h} p_4 \\ p_4' = h(\varepsilon_{\mathrm{m}} - \bar{\varepsilon}_{\mathrm{m}}) - p_2 - h_{\mathrm{n}} p_3 + \dfrac{h_{\mathrm{n}}}{h} p_4. \end{cases} \tag{55}$$

where the optimal control $v_{\mathrm{m}} = -\dfrac{1}{h} p_4$ is deduced by the stationary condition (46). The equation featuring in the system (55) is coupled with the transversality conditions

$$p_1(L) = -\mu_\Psi d_{\mathrm{r}} \zeta[u_{\mathrm{a}}(L) - \bar{u}_{\mathrm{a}}] \qquad p_2(L) = -\mu_\Psi d_{\mathrm{r}} \zeta[u_{\mathrm{m}}(L) - \bar{u}_{\mathrm{m}}], \tag{56a}$$

$$p_3(L) = -\mu_\Psi d_{\mathrm{r}}[\varepsilon_{\mathrm{a}}(L) - \bar{\varepsilon}_{\mathrm{a}}], \qquad p_4(L) = -\mu_\Psi d_{\mathrm{r}} h[\varepsilon_{\mathrm{a}}(L) - \bar{\varepsilon}_{\mathrm{a}}]. \tag{56b}$$

and with the boundary conditions on $x = 0$ (see Eqs. (20a) and (20b))

$$u_{\mathrm{a}0} = 0.0, \qquad u_{\mathrm{m}0} = 0.0, \tag{57a}$$

$$\varepsilon_{\mathrm{a}0} = 0.0, \qquad \varepsilon_{\mathrm{m}0} = 0.2\,. \tag{57b}$$

Finally, the target state, which in this case represents the "average" response in space of the system and the value that we want the state variables to assume in $x = L$, is prescribed as

$$\bar{u}_{\mathrm{a}} = \bar{\varepsilon}_{\mathrm{a}} L, \qquad \bar{u}_{\mathrm{m}} = \bar{\varepsilon}_{\mathrm{m}} L, \tag{58a}$$

$$\bar{\varepsilon}_{\mathrm{a}} = 0.1, \qquad \bar{\varepsilon}_{\mathrm{m}} = 0.0\,. \tag{58b}$$

For this particular instance of optimal control problem, we also present the numerical simulations associated with a slight alteration of the optimal problem presented beforehand, in which the exit cost functional is taken null, i.e., $\mu_\psi = 0$ and the transversality conditions reduce to $p_i = 0$, for $i = 1, 2, 3, 4$.

Results of the numerical simulations. In Fig. 2 we report the state and co-state variables obtained by solving the adhesive system while minimizing the distance from a target state (see the functional reported in Eq. (53)). In such formulation, moreover, the target state coincides with the final state of the system, which is imposed via transversality conditions. Hence, the system evolves in space, starting from the boundary conditions at $x = 0$, trying to stay the closest to these target values, both for the displacement fields and for the deformation fields, and finally trying to reach such values in $x = L$. In Fig. 2a and b we plot the displacement and the deformation fields, respectively, and their target values. Since the penalization parameters in the *running cost* are chosen as the material parameters of the system, the resulting forces associated with the *a posteriori* controllability are comparable with the ones governing the

mechanical response of the system. Hence, the displacement fields for both fibers are almost overlapping until $x = 0.5\,\mu$m; then, they start to converge toward the assigned values. In the left neighborhood of $x = L$ the reactive forces associated with the transversality conditions affect the system's behavior and alter the trajectory of the state variables, as is visible especially in Fig. 2b both for ε_{a} and for ε_{m}. The trends of the co-states reflect how well the system adheres to the transversality conditions. For p_1 and p_2, no visible alterations are present in the neighborhood of $x = L$, whereas p_3 and p_4 show a sudden decrease, or increase, respectively, as the control strengthens to impose the final state.

When the exit cost for ending up at η instead of $\bar{\eta}$ is null (see the cost functional in Eq. (53), by setting $\mu_\psi = 0$), i.e., the transversality conditions are null, the system evolves following only the minimization from the target state. As it can be seen in Fig. 3, the system follows a similar evolution to the case examined before, but, in proximity of $x = L$, the displacements do not tend to the target values, indeed u_{a} exceeds the value of $\bar{u}_{\mathrm{a}}$, while u_{m} assumes values lower than $\bar{u}_{\mathrm{m}}$, following the most natural evolution of the system.

5.4.2. Minimal elastic energy. In this second case, we want to find the control that minimizes the following functional

$$J(v) := \frac{1}{2}\mu_\Psi d_{\mathrm{r}} \left\{\zeta[u_{\mathrm{a}}(L) - \bar{u}_{\mathrm{a}}]^2 + \zeta[u_{\mathrm{m}}(L) - \bar{u}_{\mathrm{m}}]^2 + [\varepsilon_{\mathrm{a}}(L) - \bar{\varepsilon}_{\mathrm{a}}]^2 + h[\varepsilon_{\mathrm{m}}(L) - \bar{\varepsilon}_{\mathrm{m}}]^2\right\} + \frac{1}{2}\int_0^L \left\{h_{\mathrm{r}}[u_{\mathrm{a}}(x) - u_{\mathrm{m}}(x)]^2 + \varepsilon_{\mathrm{a}}^2(x) + h\varepsilon_{\mathrm{m}}^2(x) + h_{\mathrm{m}}^{(\mathrm{c})} v_{\mathrm{m}}^2(x)\right\} \mathrm{d}x, \tag{59}$$

where the exit cost for ending up at η (first summand of the right-hand side of Eq. (59)) represents the distance, with respect to a penalization, from a desired fixed state $\bar{\eta} = [\bar{u}_{\mathrm{a}}, \bar{u}_{\mathrm{m}}, \bar{\varepsilon}_{\mathrm{a}}, \bar{\varepsilon}_{\mathrm{m}}]^{\mathrm{T}}$ and the integrand function represents the normalized elastic energy density of the system plus the energy of the normalized external force $h_{\mathrm{m}}^{(\mathrm{c})} v_{\mathrm{m}} = f_{\mathrm{m}}^{(\mathrm{c})}/(k_{\mathrm{a}} d_{\mathrm{r}})$. The functional is subjected to the differential constraint given in Eq. (48) and with the integral condition of Theorem 2 satisfied exactly with $\alpha = 1$. Thus, not only the existence of the solution in guaranteed but also uniqueness. We apply the PMP to the Pontryagin's Hamiltonian function

$$H(\eta, v_{\mathrm{m}}, p) = p^\top(\mathsf{A}\eta + \mathsf{B}_{\mathrm{m}} v_{\mathrm{m}}) - \frac{1}{2}\left(\eta^\top \mathsf{Q}\,\eta + h_{\mathrm{m}}^{(\mathrm{c})} v_{\mathrm{m}}^2\right), \tag{60}$$

with the matrix Q given by

$$\mathsf{Q} = \begin{bmatrix} h_{\mathrm{r}} & -h_{\mathrm{r}} & 0 & 0 \\ -h_{\mathrm{r}} & h_{\mathrm{r}} & 0 & 0 \\ 0 & 0 & 1 & 0 \\ 0 & 0 & 0 & h \end{bmatrix}, \tag{61}$$

and the array of co-states written as $p = [p_1, p_2, p_3, p_4]^{\mathrm{T}}$, where p_1 and p_2 are non-dimensional co-states, while p_3 and p_4 have the physical units of a length. Taking into account the stationary condition for the control v_{m}

$$\frac{\partial H}{\partial v_{\mathrm{m}}}(\eta, v_{\mathrm{m}}, p) = 0 \Rightarrow -\frac{h_{\mathrm{m}}^{(\mathrm{c})}}{h} p_4 - h_{\mathrm{m}}^{(\mathrm{c})} v_{\mathrm{m}} = 0 \Rightarrow v_{\mathrm{m}} = -\frac{1}{h} p_4, \tag{62}$$

we can write the system of governing equations that solve the mechanical response of the system and the optimal problem under study

$$\begin{cases} u_{\mathrm{a}}' = \varepsilon_{\mathrm{a}} \\ u_{\mathrm{m}}' = \varepsilon_{\mathrm{m}} \\ \varepsilon_{\mathrm{a}}' = -h_{\mathrm{n}}(\varepsilon_{\mathrm{a}} - \varepsilon_{\mathrm{m}}) + h_{\mathrm{r}}(u_{\mathrm{a}} - u_{\mathrm{m}}) \\ \varepsilon_{\mathrm{m}}' = \dfrac{h_{\mathrm{n}}}{h}(\varepsilon_{\mathrm{a}} - \varepsilon_{\mathrm{m}}) - \dfrac{h_{\mathrm{r}}}{h}(u_{\mathrm{a}} - u_{\mathrm{m}}) + \dfrac{h_{\mathrm{m}}^{(\mathrm{c})}}{h^2} p_4 \\ p_1' = h_{\mathrm{r}}(u_{\mathrm{a}} - u_{\mathrm{m}}) - h_{\mathrm{r}} p_3 + \dfrac{h_{\mathrm{r}}}{h} p_4 \\ p_2' = -h_{\mathrm{r}}(u_{\mathrm{a}} - u_{\mathrm{m}}) + h_{\mathrm{r}} p_3 - \dfrac{h_{\mathrm{r}}}{h} p_4 \\ p_3' = \varepsilon_{\mathrm{a}} - p_1 + h_{\mathrm{n}} p_3 - \dfrac{h_{\mathrm{n}}}{h} p_4 \\ p_4' = h\varepsilon_{\mathrm{m}} - p_2 - h_{\mathrm{n}} p_3 + \dfrac{h_{\mathrm{n}}}{h} p_4 \end{cases} \tag{63}$$

equipped with the transversality conditions

$$p_1(L) = -\mu_\Psi d_{\mathrm{r}} \zeta [u_{\mathrm{a}}(L) - \bar{u}_{\mathrm{a}}] \qquad p_2(L) = -\mu_\Psi d_{\mathrm{r}} \zeta [u_{\mathrm{m}}(L) - \bar{u}_{\mathrm{m}}], \tag{64a}$$

$$p_3(L) = -\mu_\Psi d_{\mathrm{r}} [\varepsilon_{\mathrm{a}}(L) - \bar{\varepsilon}_{\mathrm{a}}], \qquad p_4(L) = -\mu_\Psi d_{\mathrm{r}} h [\varepsilon_{\mathrm{a}}(L) - \bar{\varepsilon}_{\mathrm{a}}]. \tag{64b}$$

We impose the boundary conditions on $x = 0$

$$u_{\mathrm{a}0} = 0.0, \qquad u_{\mathrm{m}0} = 0.0, \tag{65a}$$

$$\varepsilon_{\mathrm{a}0} = 0.0, \qquad \varepsilon_{\mathrm{m}0} = 0.2\,. \tag{65b}$$

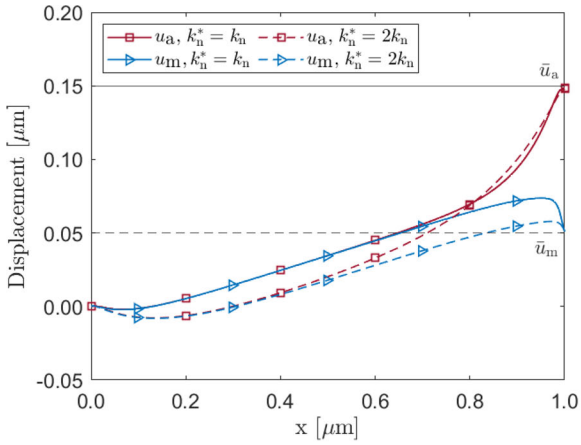
Finally, the final state is prescribed as

$$\bar{u}_{\mathrm{a}} = 0.15L, \qquad \bar{u}_{\mathrm{m}} = 0.05L, \tag{66a}$$

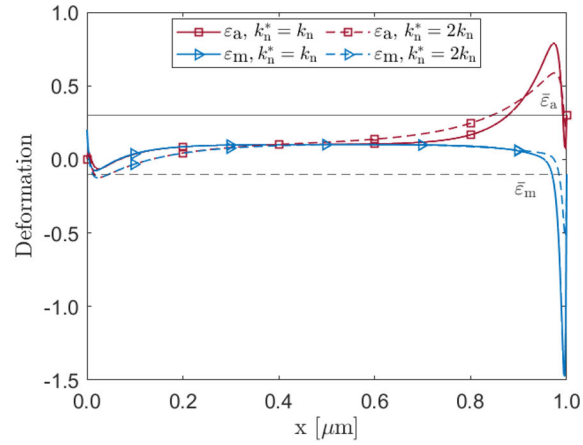
$$\bar{\varepsilon}_{\mathrm{a}} = 0.3, \qquad \bar{\varepsilon}_{\mathrm{m}} = -0.1\,. \tag{66b}$$

Results of the numerical simulations. We study the system (63) for different values of the parameter k_{n}, which is a positive material parameter that influences the magnitude of the non-elastic forces exchanged by the fibers. We consider the cases $k_{\mathrm{n}}^* = k_{\mathrm{n}}$ and $k_{\mathrm{n}}^* = 2k_{\mathrm{n}}$, where k_{n} is the reference value reported in Table 1. To this end, we remark that k_{n} features in the system of equations (63) in the non-dimensionalized constant $h_{\mathrm{n}} = k_{\mathrm{n}}/(d_{\mathrm{r}} k_{\mathrm{a}})$, so that a twofold increase in k_{n} means a twofold increase in h_{n}. The minimization of the elastic energy reduces the relative displacement between the fibers, since it minimizes the elastic part of the exchanged forces, which depends on the relative displacement $u_{\mathrm{a}} - u_{\mathrm{m}}$. In this sense, it opposes the tendency of the system to increase the relative displacement for higher values of k_{n}, although it does not avoid completely the instance. The behavior of the system can be viewed in Fig. 4a and b, in the displacement, and the deformation fields are reported, whereas in Fig. 4c the relative displacements are reported. Although the relative displacement is higher in the case $k_{\mathrm{n}}^* = 2k_{\mathrm{n}}$ than for $k_{\mathrm{n}}^* = k_{\mathrm{n}}$, in $x = L$ the transversality conditions make it so the state variables on the right boundary assume the same value, and the relative displacements are equal. The activation of the control can be viewed in the comparison between the control variable p_4 in the two cases, as reported in Fig. 4d, which experience a peak in proximity of $x = L$.

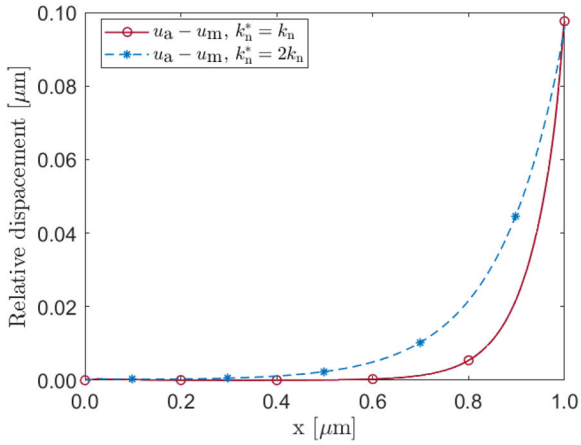
Control function v_{m}. As last result, we show in Fig. 5 the behavior of the control function $v_{\mathrm{m}} = -\dfrac{1}{h} p_4$. The latter, in particular, results to be almost homogeneous, apart from in the vicinity of the initial- and end-points of the system. In the case of the initial points, no transversality conditions are prescribed for the co-states, since the state variables are assigned on the left boundary of the system. In the proximity of the end-points, however, the value of the control function experiences an abrupt decrease due to the presence of the transversality conditions. In fact, although we do not prescribe an end-state for η (see



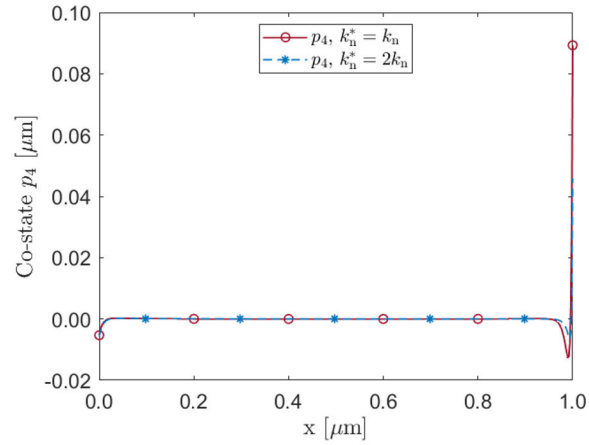
(A)
Spatial distribution of the displacements of the top and bottom fibers.



(B)
Spatial distribution of the deformations of the top and bottom fibers.



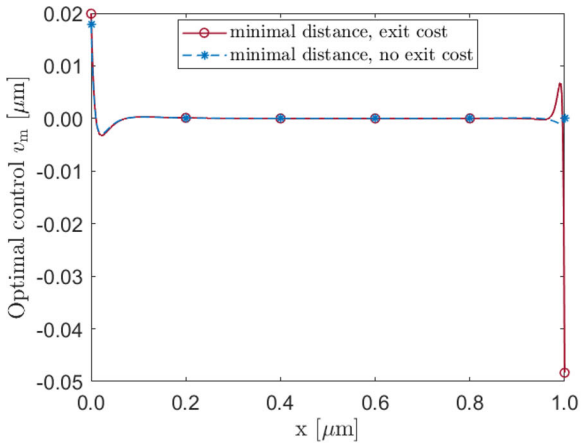
(C)
Relative displacements.



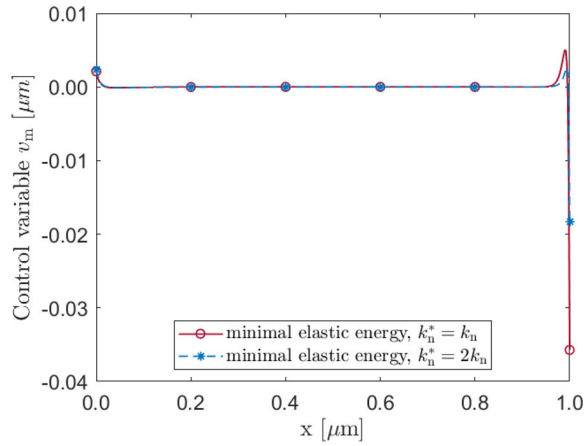
(D)
Comparison of the co-state p_4.

FIG. 4. Comparison between state variables for the minimization of the elastic energy for varying k_n (see Eq. (59))

Remark 4), we control the system through the calibration of the exit cost so that η is as close as possible to the desired state $\bar{\eta}$. This calibration, which amounts to the choice of the values of μ_Ψ and ζ, results in a severe penalization if η does not coincide with $\bar{\eta}$ on $x = L$. Hence, as it can be seen in Fig. 5a and b, the control function abruptly decreases and steers the system toward $\bar{\eta}$ as η approaches the right boundary. Notice that v_m is characterized by a natural *persistence* length, which defines how rapidly perturbations decay along the system. Since this persistence length is small, the influence of the terminal conditions imposed through the exit cost in the functional quickly propagates, ensuring that even a localized control near the boundary is sufficient for the system to reach the desired state at $x = L$. The only exception is the blue curve with asterisk markers in Fig. 5a, which refers to a case in which no exit cost is prescribed and, thus, the co-states are null at $x = L$.



(A)
Optimal controls for minimizing the distance from a target state, with and without exit cost.



(B)
Optimal controls for minimizing the elastic energy for varying values of k_{n}.

FIG. 5. Optimal controls used for the simulations, on the left for the case of minimizing the distance from a target state, with and without imposing an exit cost, on the right for the case of minimizing the total elastic energy of the adhesion complex

We remark that the procedure adopted in these simulations has the same rationale of imposing the reaction force (in terms of the transversality conditions) so that the system would go toward a constrained state, instead of imposing the constrained state and calculating the reaction force afterward.

6. Conclusions

In this work, we developed a combined approach of Continuum Mechanics and Geometric Control Theory to study space controllability of adhesive systems. In this sense, controlling a system in space means to find a suitable control function capable of driving the system itself toward a prescribed, or target, state. In particular, we start by studying the point-wise equilibrium of an adhesive system, made of two rectilinear fibers joint through an adhesive core, subjected to internal elastic and non-elastic forces. As a step forward, we conceptualize the existence of external forces which, in the framework adopted in this work, are not assigned in advance, but computed as a consequence of the system's deformation. Accordingly, we speak of *a priori* controllability when the expression of the external agencies is prescribed from the outset in order for experiments or specific phenomenologies to be reconstructed, while we refer to the *a posteriori* controllability if the external forces are not assigned but computed to bring the system to a chosen placement. Thus, we have reformulated a deformation problem within the framework of Geometric Control Theory, reinterpreting its fundamental definitions and results in terms of a spatial order parameter rather than a time-evolving dynamical variable. In parallel, we have extended the tools of Optimal Control Theory to the context of structural deformation, with the aim of designing suitable spatial controls and determining optimal deformative trajectories that satisfy prescribed optimality criteria. Two classes of optimization problems have been considered, depending on the chosen cost functional: in the first, the objective is to minimize the weighted L^2-distance between the attained configuration and a target state together with the L^2 norm of the control. In the second, the goal is to minimize the elastic energy of the structure plus the L^2 norm of the control. The corresponding necessary conditions for optimality

have been derived by applying the Pontryagin Maximum Principle (PMP), appropriately adapted to the spatial setting. Finally, a series of finite element (FEM) numerical simulations have been developed to illustrate and validate the theoretical findings, confirming the effectiveness of the proposed control framework.

Throughout our work, we mainly referred to stable focal adhesions within a purely mechanical framework, and we prove their controllability in the presence of external agents taken as part of the control functions, which may include the contributions due to chemical interactions. In this sense, our results are not immediately applied in the experimental context, since it is non-trivial to find a relation between the control functions that solve a variational problem and the chemical potential that can be associated with a spatial distribution of chemical species that evolve in time. In particular, although there are experiments in which the mechanical response is controlled by altering the chemo-mechanical enviroment by introducing some chemical species from the outset in our work we do not model the species concentration and its non-trivial coupling with the focal adhesion stress state, and we are unable to provide a comparison with existing data. However, we believe that our main result, which is the proof of the controllability of the mechanical component in focal adhesion systems, motivates further studies for the inclusion of the chemical effects in our framework.

Future investigations will cover different paths, both experimental and theoretical. From the former point of view, we would like to address the role of bio-chemistry in integrin-mediated cell–matrix systems which influence the distribution of focal adhesion and the geometry/topology of living cells. On the other hand, we want to specialize our study to the case non-homogeneous materials, even though such heterogeneity is detected at length scales lower than that of the system as a whole.

Another compelling point of future investigation concerns the study of optimal control of mechanical systems that are non-holonomic in nature and, thus, are derived from D'Alembert principle (see, e.g., [2] and references therein for a discussion on this matter). If some equivalence conditions are met, however, mechanical systems that are non-holonomic in nature can be rephrased in terms of an equivalent variational non-holonomic problem through the introduction of suitable transpositional relations, as done in [28]. In our view, this constitutes a compelling point since it would allow to rephrase an optimal control problem for non-holonomic systems within the Lagrangian formalism, in a fully variational manner.

Acknowledgements

S.D.S, A.G. and M.Z. are supported by the Italian National Group of Mathematical Physics (GNFM, INdAM). S.D.S. has been supported by PNRR MUR project PE0000023-NQSTI and by INDAM, in the context of "Bando di concorso a n. 45 mensilitá di Borse di studio per l'estero." M.Z. acknowledges the project "Mathematics for Industry 4.0" 2020F3NCPX PRIN2020 funded by the Italian MUR, S.D.S and M.Z have been supported by the PRIN 2022 PNRR project *Innovative multiscale approaches, possibly based on Fractional Calculus, for the effective constitutive modeling of cell mechanics, engineered tissues and metamaterials in Biomedicine and related fields* P2022KHFNB. A. G. has been supported by the Research Project Prin2022 PNRR of National Relevance "CORTIS" (Grant No. 2022TWKA72).

Author contributions All the authors have contributed equally.

Funding Open access funding provided by Università degli Studi di Bari Aldo Moro within the CRUI-CARE Agreement.

Data availability No datasets were generated or analyzed during the current study.

Declarations

Conflict of interest The authors declare no conflict of interest.

Open Access. This article is licensed under a Creative Commons Attribution 4.0 International License, which permits use, sharing, adaptation, distribution and reproduction in any medium or format, as long as you give appropriate credit to the original author(s) and the source, provide a link to the Creative Commons licence, and indicate if changes were made. The images or other third party material in this article are included in the article's Creative Commons licence, unless indicated otherwise in a credit line to the material. If material is not included in the article's Creative Commons licence and your intended use is not permitted by statutory regulation or exceeds the permitted use, you will need to obtain permission directly from the copyright holder. To view a copy of this licence, visit http://creativecommons.org/licenses/by/4.0/.

Publisher's Note Springer Nature remains neutral with regard to jurisdictional claims in published maps and institutional affiliations.

Appendix A: Spectral and geometric properties of the matrix A

In this appendix, we analyze the key spectral properties of the matrix A reported in Eq. (16) and encoding the structural behavior of the adhesive system discussed in this work.

We note that A has the following eigenvalues

$$\lambda_1 = 0, \tag{67a}$$

$$\lambda_2 = -\frac{h_{\mathrm{n}}(1+h) + \sqrt{1+h}\sqrt{h_{\mathrm{n}}^2 + hh_{\mathrm{n}}^2 + 4hh_{\mathrm{r}}}}{2h}, \tag{67b}$$

$$\lambda_3 = -\frac{h_{\mathrm{n}}(1+h) - \sqrt{1+h}\sqrt{h_{\mathrm{n}}^2 + hh_{\mathrm{n}}^2 + 4hh_{\mathrm{r}}}}{2h}, \tag{67c}$$

computed as the roots of the characteristic polynomial

$$p(\lambda) = \lambda^4 + \left(1 + \frac{1}{h}\right) h_{\mathrm{n}}\lambda^3 - \left(1 + \frac{1}{h}\right) h_{\mathrm{r}}\lambda^2, \tag{68}$$

with λ_1, λ_2 and λ_3 having algebraic multiplicity $m_1 = 2$, $m_2 = 1$ and $m_3 = 1$, respectively, since λ_1 is a double solution of the algebraic equation $p(\lambda) = 0$. To investigate the geometric multiplicity μ_i of each eigenvalue λ_i, with $i = 1, 2, 3$, we consider the dimension of the eigenspace $\mathcal{V}_i$ associated with λ_i. In particular, we solve the linear problems $(\mathsf{A} - \lambda_1\mathsf{I})\eta = \mathsf{A}\eta = \mathbf{0}$, $(\mathsf{A} - \lambda_2\mathsf{I})\eta = \mathbf{0}$ and $(\mathsf{A} - \lambda_3\mathsf{I})\eta = \mathbf{0}$, whose spaces of solutions, i.e., the eigenspaces $\mathcal{V}_1$, $\mathcal{V}_2$ and $\mathcal{V}_3$ associated with λ_i, λ_2 and λ_3, respectively, are given by

$$\mathcal{V}_1 = \mathrm{span}\{(1, 1, 0, 0)\}, \tag{69a}$$

$$\mathcal{V}_2 = \mathrm{span}\left\{\left(-\frac{h}{\lambda_2}, \frac{1}{\lambda_2,}, -h.1\right)\right\}, \tag{69b}$$

$$\mathcal{V}_3 = \mathrm{span}\left\{\left(-\frac{h}{\lambda_3}, \frac{1}{\lambda_3,}, -h.1\right)\right\}, \tag{69c}$$

and with I being the fourth-order identity matrix. Moreover, $\mu_1 = \dim\mathcal{V}_1 = 1 < m_1$, while $\mu_2 = \dim\mathcal{V}_2 = 1 = m_2$ and $\mu_3 = \dim\mathcal{V}_3 = 1 = m_3$. Hence, since the algebraic multiplicity of λ_1 is different from the geometric one, the matrix A cannot be diagonalized but, since all the eigenvalues are real numbers, its

canonic Jordan form is well defined. Accordingly, we introduce the upper triangular block matrix J

$$\mathsf{J} = \begin{bmatrix} \lambda_1 & 1 & 0 & 0 \\ 0 & \lambda_1 & 0 & 0 \\ 0 & 0 & \lambda_2 & 0 \\ 0 & 0 & 0 & \lambda_3 \end{bmatrix}, \tag{70}$$

and a non-singular matrix P such that $\mathsf{J} = \mathsf{P}^{-1}\mathsf{A}\mathsf{P}$. To construct P, we consider the generalized eigenvectors associated with λ_1. To start with, let us compute $\mathcal{V}_1^{(2)}$ as the space of the solutions of the linear problem $(\mathsf{A} - \lambda_1 \mathsf{I})^2 \eta = \mathsf{A}^2 \eta = \mathbf{0}$, thereby obtaining

$$\mathcal{V}_1^{(2)} = \text{span}\{(1,1,0,0),(0,0,1,1)\}. \tag{71}$$

By looking at the definition of $\mathcal{V}_1^{(2)}$, we take as first generalized eigenvector of A associated with λ_1 the vector $\eta_2 = (0,0,1,1)$, since $\eta_2 \in \mathcal{V}_1^{(2)}/\mathcal{V}_1$, while the second generalized eigenvector of A relative to λ_1 is obtained as $(\mathsf{A} - \lambda_1 \mathsf{I})\eta_2 = \mathsf{A}\eta_2 = (1,1,0,0)$. Finally, we have

$$\mathsf{P} = \begin{bmatrix} 1 & 0 & -\frac{h}{\lambda_2} & -\frac{h}{\lambda_3} \\ 1 & 0 & \frac{1}{\lambda_2} & \frac{1}{\lambda_3} \\ 0 & 1 & -h & -h \\ 0 & 1 & 1 & 1 \end{bmatrix}. \tag{72}$$

Appendix A.1: Equilibria and their stability

We now examine the equilibrium points of the matrix A and the conditions under which they are stable or instable.

We recall that the point $\eta^{(\text{eq})} \in \mathbb{R}^4$ is an equilibrium state for the differential system in Eq. (18) if the constant function $\eta(t) = \eta^{(eq)}$ is a solution. In particular, since the matrix A is independent on the order parameter x and no source term is present, the search for equilibrium states requires to solve the linear system of algebraic equations

$$\mathsf{A}\eta = \mathbf{0}. \tag{73}$$

In other words, the equilibrium states of the differential system in Eq. (18) are the only solutions of Eq. (73). Since the matrix A is singular, the equilibrium states define a vector subspace $\mathcal{E} \subset \mathbb{R}^4$ of $\mathbb{R}^4$ of dimension one, because the rank of A is equal to three. In detail, we have

$$\mathcal{E} = \text{span}\{(1,1,0.0)\}. \tag{74}$$

Finally, since the eigenvalue λ_3 of A is strictly positive, independently of the choice of the material parameters, standard results of the spectral theory of linear systems' stability ensure that all the equilibrium points are instable.

Appendix A.2: Analytical solution

The solution of the ordinary differential equations reported in Eq. (18) can be computed analytically. This way, by exploiting the formalism of the exponential matrix, we can write the solution $\boldsymbol{\eta} : [0, L] \to \mathbb{R}^4$ as

$$\eta(x) = \mathrm{e}^{x\mathsf{A}} c_0 = \mathsf{P}\mathrm{e}^{x\mathsf{J}}\mathsf{P}^{-1} c_0, \tag{75}$$

where

$$\mathrm{e}^{x\mathsf{J}} = \begin{bmatrix} \mathrm{e}^{x\lambda_1} & x\mathrm{e}^{x\lambda_1} & 0 & 0 \\ 0 & \mathrm{e}^{x\lambda_1} & 0 & 0 \\ 0 & 0 & \mathrm{e}^{x\lambda_2} & 0 \\ 0 & 0 & 0 & \mathrm{e}^{x\lambda_3} \end{bmatrix} \tag{76}$$

and $c_0 = \mathsf{P}[c_1, c_2, c_3, c_4]^{\mathrm{T}}$ is the array of integration constants. Finally, we have

$$\eta(x) = \mathsf{P}\mathrm{e}^{x\mathsf{J}}[c_1, c_2, c_3, c_4]^{\mathrm{T}}, \tag{77}$$

leading to

$$u_{\mathrm{a}}(x) = c_1 + c_2 x - hc_3 \frac{\mathrm{e}^{\lambda_2 x}}{\lambda_2} - hc_4 \frac{\mathrm{e}^{\lambda_3 x}}{\lambda_3}, \tag{78}$$

$$u_{\mathrm{m}}(x) = c_1 + c_2 x + c_3 \frac{\mathrm{e}^{\lambda_2 x}}{\lambda_2} + c_4 \frac{\mathrm{e}^{\lambda_3 x}}{\lambda_3} \tag{79}$$

$$\varepsilon_{\mathrm{a}}(x) = c_2 - h[c_3 \mathrm{e}^{\lambda_2 x} + c_4 \mathrm{e}^{\lambda_3 x}], \tag{80}$$

$$\varepsilon_{\mathrm{m}}(x) = c_2 + c_3 \mathrm{e}^{\lambda_2 x} + c_4 \mathrm{e}^{\lambda_3 x}. \tag{81}$$

Appendix B: Pontryagin Maximum Principle (PMP) for linear systems

The PMP applied to first-order, linear systems of ODEs states the following constrained optimization problem

$$\min_{v(\cdot)} \; J(v) = \frac{1}{2}\hat{\Psi}(\eta(L), L) + \frac{1}{2}\int_0^L \hat{\ell}(\eta(x), v(x), x)\,\mathrm{d}x, \tag{82a}$$

$$\text{subject to} \quad \boldsymbol{\eta}' = \mathsf{A}\eta + \mathsf{B}v, \qquad \eta(0) = \eta_0, \tag{82b}$$

whose solution is the array of controls $v^* \in L^\infty([0, L], \mathbb{R}^M)$ that minimizes the functional J and drives the space evolution of the state variables η^*, solution of the linear system in Eq. (82b). In particular, the smooth function

$$\hat{\Psi} : \mathbb{R}^M \times \mathbb{R} \to \mathbb{R}, \quad \text{s.t.} \quad \Psi(L) := \hat{\Psi}(\eta(L), L), \tag{83}$$

which is supposed to be positive, (see [34] for the details) is the *cost for ending up* at state η and

$$\hat{\ell} : \mathbb{R}^N \times \mathbb{R}^M \times \mathcal{B} \to \mathbb{R}, \tag{84}$$

is a smooth function called *running cost*. A specific form of Ψ and $\hat{\ell}$ is chosen accordingly to the physical situation accounted for, and some examples will be given in the following.

The optimal control solution v^* of the minimization problem in Eqs. (82a) and (82b) and the corresponding optimal trajectory η^* satisfy the following necessary conditions

(i) Hamiltonian system

Defined the so-called Pontryagin's Hamiltonian function

$$\hat{H} : \mathbb{R}^N \times \mathbb{R}^M \times \mathbb{R}^N \times \mathcal{B} \to \mathbb{R}, \tag{85}$$

and setting

$$\hat{H}(\eta, v, p, x) = p^{\top}(\mathsf{A}\eta + \mathsf{B}v) - \ell(\eta, v, x),$$

there exists a non-trivial array of smooth (adjoint) co-states $p : \mathcal{B} \to \mathbb{R}^N$ such that

$$\boldsymbol{\eta}^{*'} = \frac{\partial \hat{H}}{\partial p}(\eta^*, v^*, p, x) = \mathsf{A}\eta^* + \mathsf{B}v^*, \tag{86a}$$

$$\boldsymbol{p}' = -\frac{\partial \hat{H}}{\partial \eta}(\eta^*, v^*, p, x) = -\mathsf{A}^\top p + \frac{\partial \hat{\ell}}{\partial \eta}(\eta^*, v^*, p, x). \tag{86b}$$

Informally, the PMP states that the Pontryagin's Hamiltonian H must necessarily reach an extremum among all admissible controls. Whether this extremum is a maximum or a minimum depends on the problem and on the sign convention used in defining H itself.

(ii) Stationary condition

For almost every $x \in \mathcal{B}$, the optimal control minimizes the Hamiltonian:

$$\frac{\partial \hat{H}}{\partial v}(\eta^*(x), v^*(x), p(x), x) = 0,$$

which can be used to yield a feedback relation between v^* and p.

(iii) Transversality conditions

Let the final state $\eta(L)$ be free (unconstrained terminal state), then the transversality condition is

$$p(L) = -\frac{\partial \hat{\Psi}}{\partial \eta}(\eta(L), L). \tag{87}$$

Remark 4. Notice that it is possible also to constrain the final state to be a prescribed one, i.e., $\eta(L) = \eta_L$. In this case $p(L)$ is not fixed and is left free, representing the Lagrange multiplier associated with the terminal equality constraint $\eta(L) = \eta_L$.

References

[1] Balaban, N.Q., Schwarz, U.S., Riveline, D., Goichberg, P., Tzur, G., Sabanay, I., Mahalu, D., Safran, S., Bershadsky, A., Addadi, L., Geiger, B.: Force and focal adhesion assembly: a close relationship studied using elastic micropatterned substrates. Nat. Cell Biol. **3**(5), 466–472 (2001)

[2] Bloch, A.: Nonholonomic Mechanics and Control. Springer, New York, NY (2015)

[3] Cao, X., Ban, E., Baker, B.M., Lin, Y., Burdick, J.A., Christopher, C.S., Shenoy, V.B.: Multiscale model predicts increasing focal adhesion size with decreasing stiffness in fibrous matrices. Proc. Natl. Acad. Sci. **114**, 23 (2017)

[4] Cao, X., Lin, Y., Driscoll, T.P., Barraza, J.F., Cukierman, E., Mauck, R.L., Shenoy, V.B.: A chemomechanical model of matrix and nuclear rigidity regulation of focal adhesion size. Biophys. J . **109**(9), 1807–1817 (2015)

[5] Choquet, D., Felsenfeld, D.P., Sheetz, M.P.: Extracellular matrix rigidity causes strengthening of integrin–cytoskeleton linkages. Cell **88**(1), 39–48 (1997)

[6] Coron, J.-M.: Control and Nonlinearity. Mathematical Surveys and Monographs, AMS, Providence, RI (2007)

[7] Cox, H.L.: The elasticity and strength of paper and other fibrous materials. Br. J. Appl. Phys. **3**(3), 72 (1952)

[8] Deshpande, V., Mrksich, M., McMeeking, R., Evans, A.: A bio-mechanical model for coupling cell contractility with focal adhesion formation. J. Mech. Phys. Solids **56**(4), 1484–1510 (2008)

[9] Di Stefano, S., Benvenuti, E., Coscia, V.: On the role of friction and remodelling in cell–matrix interactions: a continuum mechanical model. Int. J. Non-Linear Mech. **142**, 103966 (2022)

[10] Di Stefano, S., Florio, G., Napoli, G., Pugno, N.M., Puglisi, G.: On the role of elasticity in focal adhesion stability within the passive regime. Int. J. Non-Linear Mech. **146**, 104157 (2022)

[11] Di Stefano, S., Zoppello, M.: A priori and a posteriori controllability of volumetric growth: a theoretical approach. Z. Angew. Math. Phys. **76**(6), 1–27 (2025)

[12] DiCarlo, A., Quiligotti, S.: Growth and balance. Mech. Res. Commun. **29**(6), 449–456 (2002)

[13] Dillard, D.A.: Fundamentals of stress transfer in bonded systems. Adhes. Sci. Eng. **1**, 1–44 (2002)

[14] Ebnesajjad, S., Landrock, A.H.: Adhesives Technology Handbook. William Andrew, New York (2014)

[15] Epstein, M., Maugin, G.A.: Thermomechanics of volumetric growth in uniform bodies. Int. J. Plast **16**(7–8), 951–978 (2000)

[16] Grillo, A., Di Stefano, S.: An a posteriori approach to the mechanics of volumetric growth. Math. Mech. Complex Syst. **11**(1), 57–86 (2023)

[17] Grillo, A., Di Stefano, S.: A formulation of volumetric growth as a mechanical problem subjected to non-holonomic and rheonomic constraint. Math. Mech. Solids **28**(10), 2215–2241 (2023)

[18] Jurdjevic, V.: Geometric Control Theory. Cambridge University Press, Cambridge (1997)

[19] Kendall, K.: Molecular Adhesion and its Applications: The Sticky Universe. Springer, Cham (2001)

[20] Lanczos, C.: The Variational Principles of Mechanics. Dover Publications Inc, Mineola, NY (1970)
[21] Lodish, H.F.: Molecular Cell Biology. Macmillan, London (2008)
[22] Ma, Q., Rejab, M., Siregar, J., Guan, Z.Z.: A review of the recent trends on core structures and impact response of sandwich panels. J. Compos. Mater. **55**(18), 2513–2555 (2021)
[23] Maggistro, R., Zoppello, M.: Optimal motion of a scallop: some case studies. IEEE Control Syst. Lett. **3**(4), 841–846 (2019)
[24] Marchello, R., Morandotti, S., H., Zoppello, M.: The N-link swimmer in three dimensions: controllability and optimality results. Acta Appl. Math. **178**(6), 25 (2022)
[25] Pugno, M.N., Carpinteri, A.: Tubular adhesive joints under axial load. J. Appl. Mech. **70**(6), 832–839 (2003)
[26] Nicolas, A., Geiger, B., Safran, S.A.: Cell mechanosensitivity controls the anisotropy of focal adhesions. Proc. Natl. Acad. Sci. **101**(34), 12520–12525 (2004)
[27] Pandey, N., Soto-Garcia, L.F., Liao, J., Zimmern, P., tNguyen, K., Hong, Y.: Mussel-inspired bioadhesives in healthcare: design parameters, current trends, and future perspectives. Biomat. Sci. **8**(5), 1240–1255 (2020)
[28] Pastore, A., Giammarini, A., Grillo, A.: Reconciling Kozlov's vakonomic method with the traditional non-holonomic method: solution of two benchmark problems. Acta Mech. **235**(4), 2341–2379 (Jan.2024)
[29] Pompe, T., Kaufmann, M., Kasimir, M., Johne, S., Glorius, S., Renner, L., Bobeth, M., Pompe, W., Werner, C.: Friction-controlled traction force in cell adhesion. Biophys. J . **101**(8), 1863–1870 (2011)
[30] Puglisi, G., Truskinovsky, L.: Cohesion-decohesion asymmetry in geckos. Phys. Rev. E-Stat. Nonlinear Soft Matter Phys. **87**(3), 032714 (2013)
[31] Pugno, N.M., Yin, Q., Shi, X., Capozza, R.: A generalization of the coulomb's friction law: from graphene to macroscale. Meccanica **48**(8), 1845–1851 (2013)
[32] Schwarz, U., Balaban, N., Riveline, D., Bershadsky, A., Geiger, B., Safran, S.: Calculation of forces at focal adhesions from elastic substrate data: The effect of localized force and the need for regularization. Biophys. J . **83**(3), 1380–1394 (2002)
[33] Shemesh, T., Geiger, B., Bershadsky, A.D., Kozlov, M.M.: Focal adhesions as mechanosensors: a physical mechanism. Proc. Natl. Acad. Sci. **102**(35), 12383–12388 (2005)
[34] Trélat, E.: Contrôle Optimal: Théorie & Applications, vol. 36. Vuibert, Paris (2005)
[35] Tserpes, K., Barroso-Caro, A., Carraro, P.A., Beber, V.C., Floros, I., Gamon, W., Kozłowski, M., Santandrea, F., Shahverdi, M., Skejić, D., et al.: A review on failure theories and simulation models for adhesive joints. J. Adhes. **98**(12), 1855–1915 (2022)
[36] Vinson, J.R.: The Behavior of Sandwich Structures of Isotropic and Composite Materials. Routledge, London (2018)
[37] Volkersen, O.: Die nietkraftverteilung in zugbeanspruchten nietverbindungen mit konstanten laschenquerschnitten. Luftfahrtfor Schung **15**, 41–47 (1938)
[38] Xiao, Z., Qixuan, Z., Niu, Y., Zhao, D.: Adhesion advances: from nanomaterials to biomimetic adhesion and applications. Soft Matter **18**(18), 3447–3464 (2022)

Salvatore Di Stefano
Dipartimento di Matematica
Universitá degli Studi "Aldo Moro" di Bari
via Edoardo Orabona, 4
70125 Bari
Italy
e-mail: salvatore.distefano@uniba.it

Alessandro Giammarini
Dipartimento di Ingegneria Civile e Ambientale
Politecnico di Milano
Piazza Leonardo da Vinci 32
20133 Milano MI
Italy
e-mail: alessandro.giammarini@polimi.it

Marta Zoppello
Dipartimento di Scienze Matematiche "Giuseppe Luigi Lagrange"
Politecnico di Torino
corso Duca degli Abruzzi, 24
10129 Torino
Italy
e-mail: marta.zoppello@polito.it

Communicated by Salvatore Di Stefano

(Received: November 11, 2025; revised: April 23, 2026; accepted: May 15, 2026)